UNIVERSITÀ
DEGLI STUDI
DI PADOVA

UNIVERSITÀ DEGLI STUDI DI PADOVA

ENGINEERING INDUSTRIAL DEPARTMENT

MASTER DEGREE IN CHEMICHAL AND INDUSTRIAL PROCESS ENGINEERING

Master thesis in
Chemical and Industrial Process Engineering

ANALYSIS AND CHARACTERIZATION OF HIGH LOADING NANOFLUID ELECTROLYTES FOR REDOX FLOW BATTERY FOR ELECTRICAL VEHICLES

Supervisor: Ing. Monica Giomo

Candidate: ALBERTO GIURIATTI

ACADEMIC YEAR 2017-2018

Abstract

This Thesis is the first step of a project which has the aim to develop a new battery based on redox flow battery technology using a suspension of electroactive nanoparticle dispersed in a liquid medium. Nanofluids permits to overcome solubility limitations, reduce the viscosity due to the small particle size and to exploit the advantages of redox flows battery.
The aim of the Thesis is to develop two nanofluids, one for the anodic process and one for the cathodic one.
The nanofluids developed are based on 2 different material: TiO_2 and LMNO.
Both solid active materials have a modified surface which permits to decrease the viscosity due to the negative layer coverage which create a repulsive force between particles.
The nanofluids developed are based on propylene carbonate solvent with $LiClO_4$ which guaranties a wide range of stability.
Electrochemical and rheological test has been performed on the nanofluids.
The surface-modified TiO_2 particles retain the electrochemical activity and the intercalation process shows higher activity than the deintercalation one due to the negative layer around the particle which attract the lithium ion near the surface.
Electrochemical properties of pristine and surface-modified TiO_2 have been evaluated by Cyclic voltammetry and the mechanisms of lithium intercalation process have been investigated
A chronoamperometry test has been performed for modified and pristine material. TiO_2 modified provides a 58% higher current than that of the pristine, with the same energy spent for mixing, confirming that the surface treatment increases the performance of nanofluid.
Lithium in LMNO has been discharge with a new procedure to permits the surface treatment.
The procedure allowed to partially discharge the lithium present in the material, making the surface treatment possible.
The overall LMNO modification process causes an increase in the viscosity of nanofluid and turn off the electrochemical particle activity. An attempt to explain the nanofluid behaviour is proposed.

Riassunto

Questa Tesi è il primo passo di un progetto che ha lo scopo di sviluppare una nuova batteria basata sulla tecnologia delle batterie a flusso redox utilizzando una sospensione di nanoparticelle elettroattive in un mezzo liquido. I nanofluidi consentono di superare i limiti di solubilità, ridurre la viscosità a causa delle piccole dimensioni delle particelle e sfruttare i vantaggi della batteria a flusso redox.

Lo scopo della tesi è quello di sviluppare due nanofluidi, uno per il processo anodico e uno per quello catodico.

I nanofluidi sviluppati si basano su 2 materiali diversi: TiO_2 e LMNO.

Entrambi i materiali hanno una superficie modificata che consente di ridurre la viscosità essendo rivestita da uno strato negativo che crea una forza repulsiva tra le particelle.

I nanofluidi sviluppati sono basati sul carbonato di propilene con $LiClO_4$ che garantisce un'ampia finestra di stabilità.

Sono stati eseguiti test elettrochimici e reologici sui nanofluidi.

Le particelle TiO_2 modificate in superficie mantengono l'attività elettrochimica e il processo di intercalazione mostra un'attività più elevata di quella di deintercalazione dovuta allo strato negativo attorno alla particella che attira lo ione litio vicino alla superficie.

Le proprietà elettrochimiche di TiO_2 pura e della TiO_2 modificata in superficie sono state valutate mediante voltammetria ciclica e sono stati studiati i meccanismi del processo di intercalazione del litio.

È stato eseguito un test cronoamperometrico sia per il materiale modificato che per il puro. La TiO_2 modificata fornisce una corrente superiore del 58% rispetto a quella pura, con la stessa energia spesa per la miscelazione, confermando che il trattamento superficiale aumenta le prestazioni elettrochimiche del nanofluido.

Il litio nel LMNO è stato scaricato con una nuova procedura per consentire il trattamento superficiale.

La procedura ha permesso di scaricare parzialmente il litio presente nel materiale, rendendo possibile il trattamento superficiale.

Il processo di modificazione del LMNO completo causa un aumento della viscosità del nanofluido e spegne l'attività elettrochimica delle particelle. Viene proposta una spiegazione di questo comportamento.

Table of contents

Introduction

The electrical mobility is a great challenge in our society and the demand of new solutions has been increased in the last years.
The main technology used to accumulate the energy in electrical vehicles is Li-ion battery. This battery is expensive, it needs a long time to be charged and it does not provide a high autonomy.
A redox flow battery with nanofluid has been recognized as a promising alternative technology.
Nanofluid is a suspension of nanoparticle in a liquid medium. Using nanofluid it is possible to overcome solubility limitations and obtain a low viscosity due to the small size of particles.
This permits to exploit the advantages of redox flow configuration, which permits to decoupling the power and capability.
This Thesis represents the first step of the project.
The aim of the Thesis is to develop and characterize two new nanofluids, one for the anodic process and one for the cathodic one.
This work is divided in four chapters.
In the Chapter 1, RFB systems which exploit solid electroactive material are presented. Attention is focused on configurations, materials and mixing techniques used in the technologies reported in literature.
There are four different ways to exploit the high energy density of solid in a redox flow battery: a) flowing carbon as electrochemical reaction electrodes, b) flowing solid active materials with flowing carbon conducting, c) flowing active material particles colliding on current collectors without carbon and d) targeted redox mediators as the power carriers with static solid active materials providing energy storage.
Several lithium-based materials have been taken into account examinating their advantages and disadvantages.
Different ways to pump and to move fluid have been considered, for example intermitted flow, gravimetric flow and the magnetic pumping.
In Chapter 2 the most performant nanofluids available in literature have been presented.
The development of a new non-aqueous lithium based nanofluid has been described. The proposed approach is based on a useful surface treatment, proposed in literature, which allows to obtain nanofluids with low viscosity, retaining good electrochemical properties.
In Chapter 3, the materials used and methods adopted in this work are described. The chapter is divided in four section: nanofluids preparation, cycling voltammetry, chronoamperometry and viscosity measurement. For each section the materials and methods are described in details.
In the Chapter 4, the results of this work have been reported.

The electrochemical behavior and the rheological properties of the developed nanofluids have been evaluated. A comparison between the surface modified material and the pristine one has been done and the mechanism of intercalation/deintercalation in redox flow system has been investigated. The suitability of the adopted procedure has been evaluated.

Chapter 1

High Energy Redox Flow Battery

This chapter starts discussing how a battery works and what its main features. Attention is focused on redox flow batteries (RFBs) to assess their potential as a power source for electric vehicles. An overview of RFB systems with solid material is reported.
It is divided into three sections: design flow, active material and flow/agitation method. The analysis permits to better understand how solid is used in RFBs and why it allows to obtain an high energy density. Advantages and disadvantages of RFBs are underlined.

1.1 Battery

Batteries store electrical energy within chemical components of different electrochemical potentials. The difference of these potential determines the battery voltage. A wide variety of batteries has been developed depending on the application for several voltages, capacities, power densities, costs, etc.
As shown in Figure 1.1, a battery consists of current collectors for the transport of electrons to and from the external circuit, an anode (negative electrode), a cathode (positive electrode), and an electrolyte to provide ionic transport between cathode and anode through a separator which is necessary to maintain charge neutrality during charge/discharge.
The ions from the oxidation reaction (red→ox) at the anode are transferred to cathode where reduction (ox→red) occurs during the discharging process and vice versa in the charging process. The total charge capacity is determined by the type and amount of active materials in the electrolytes.
Another similar type of electrical energy storage device is the supercapacitor that store electrical energy within the electrical double layer near the surface of the electrode. In this type of device, the redox reactions are not required.
Solid batteries must be connected in various combinations of parallel and series configurations to provide the desired output current/voltage. This causes high costs due to the additional auxiliary equipment and typically the need for a heat removal system which also adds significant weight.
One promising approach is high energy density RFB, which permits to simplify battery system design thanks to the decoupling of power and capability.

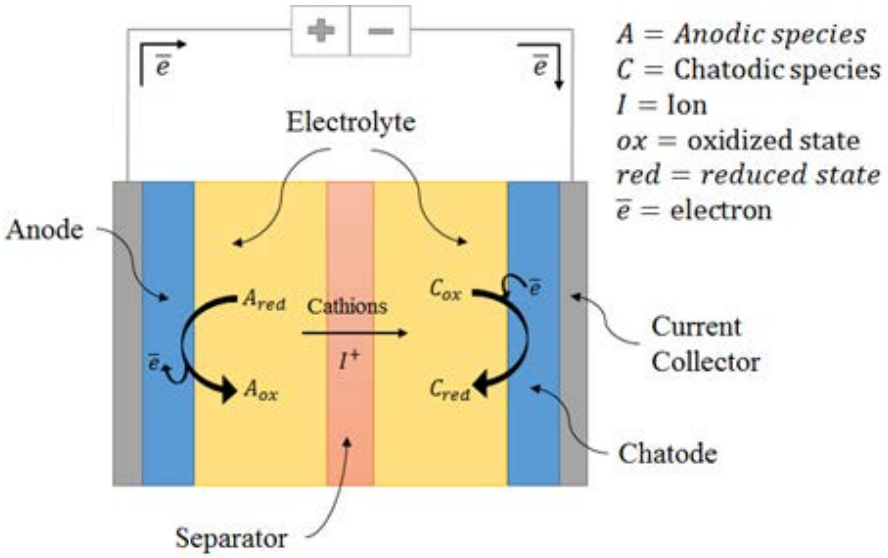

Figure 1.1 *Simplified scheme of conventional battery during discharging process. The direction of arrow are inverted in the charging process.*

1.2 Redox Flow Battery (RFB)

As shown in Figure 1.2, a typical RFB is composed by two power electrochemical cells with porous electrodes separated by ion-selective and ion-conductive membrane. It includes storage tanks containing electrolyte with the desired amount of dissolved redox and a pumping system to connect the cells to storage tanks.

During battery operation, the electrolytes are pumped through the electrochemical cells to oxidize/reduce the electroactive specie. In the anodic and cathodic compartments, the reactions occur at the surface of the porous electrodes. In this system, battery capacity is decoupled from

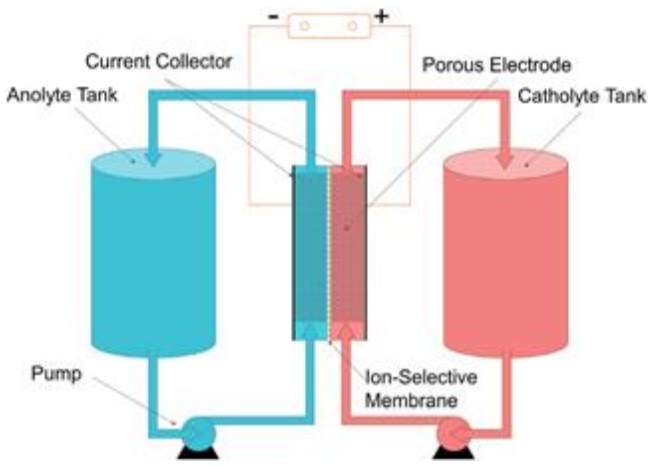

Figure 1.2 *Standard structure of conventional RFB with 2 tanks, porous electrodes and pumps. (Qi and Koenig, 2017)*

power because the first depends on the dimension of the storage tanks while the second on the performance of cells reaction.

1.3 RFB with solid material for the transport industry

The main parameters for the transport application are the energy density and the energy lost in the pumping operation. The first is a measure of how much energy the battery can store, in a given mass: it is based on both the mass of the energy store and the volume of the storage facility. The second is determined principally by the viscosity of solution and by the structure of the electrode (porous, honeycomb etc).

Commercial systems such as vanadium RFB (VRFB) have reported energy density around of 25-50 Wh L^{-1} which is low in comparison to Li-ion battery that reports about 250-693 Wh L^{-1} (en.wikipedia.org/wiki/Lithium-ion_battery). The root causes of the relatively low energy density for conventional RFBs are the following: 1) limited cell voltages due to the narrow electrolyte stability window and 2) low volumetric capacity due to solubility limits of the redox compounds.

The electrolyte stability window is limited because the solvent for conventional RFBs is water, and the thermodynamic stability range is 1.23 V. To improve RFB operating voltages, water has to be replaced with organic solvents having higher stability windows. In addition, a couple of redox compounds that are highly soluble within organic solvent and giving higher differential of potential as possible have to be selected. However, the cost and flammability of organic RFB systems could be a limit for the transport application.

The second limitation is electroactive material solubility and it is a challenge for both aqueous and organic RFBs. The number of electrons that can be exchanged for a given volume or mass of electrolyte is proportional to concentration of redox compounds, so also with energy density. To solve this limit the use of solid material has proven to be the best solution due to the high intrinsic energy density of solid instead of liquid. In particular, one increasingly popular approach consists of insoluble solid particles dispersed in liquid medium that they deliver the energy through the redox reactions or double layer stored (supercapacitor). As it is shown in Figure 1.3, nano or micrometer particles are dispersed in a liquid phase.

In this way the first limit, solubility, is avoided but the viscosity of the electrolyte increases very quickly due to the collisions between particles and against the wall of the cell structure.

In order to represent an alternative for transport industry, the energy density of RFB should not be necessary higher than Li-ion battery, but the battery has to be more convenient considering cost and performance.

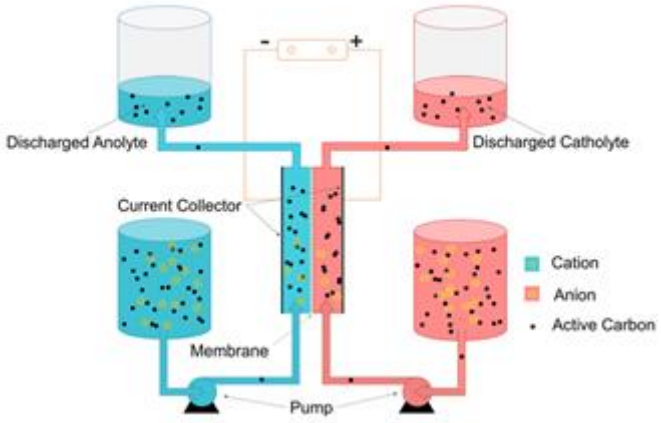

Figure 1.3 *General representation of RFB based on solid suspension electrolyte. (Qi and Koenig, 2017)*

The main characteristic of RFB is the decoupling of power and energy storage. The cost of realization of cell is generally higher than the realization of tanks, so over a specific critical battery size the RFB could cost less than Li-ion battery or other solid static batteries.
Currently, the RFB is not applicable as on-board source in electric vehicles because the critical size is too high, but with a significant increasing of energy density, the critical size decreases and this technology could become a real alternative.
Obviously, a minimum value of energy density remains a constraint for the transport industry to ensure an acceptable autonomy to the vehicle.
The laboratory-scale studies on RFB with solid material available in literature refer to several system design, different active material and some operation mode.
The following classification is suggested by Qi and Koenig (2017).

1.3.1 System Design

A lot of different innovative engineering designs have been developed managing two-phase (solid and liquid) system. They could be segment into four main groups, dependent on the flowing conditions and the role of carbon in the electrolyte which is widely used due to its high conductivity and low density.
The segments are the following: 1) flowing carbon as the electrochemical reaction electrodes, 2) flowing solid active materials within a carbon conducting network, 3) flowing active material particles colliding on current collectors without carbon, and 4) soluble redox mediators for power with solid active materials within tanks for energy. An explanation about these designs has been done in the following paragraphs.

1.3.1.1 I: Flowing carbon as electrochemical reaction electrodes

The carbon nano/microsized particles are dispersed in liquid electrolyte and it flows in the electrochemical cells as shows in Figure 1.4. For this type of flow, the added particles to the electrolyte are not themselves the electroactive material undergoing redox chemistry, but they improve the rate or utilization of the redox chemistry that occurs within the electrolyte.

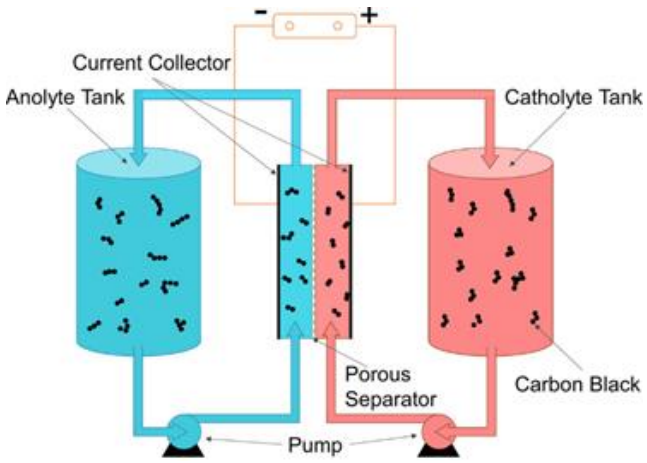

Figure 1.4 *Simplified representation of RFB with carbon network. Cation and Anion work as redox species and carbon works as support and conductive network. (Qi and Koenig, 2017)*

These carbon particles form percolated aggregates and electrochemical reactions occur on the surface while it is in contact with the current collector.

This design could result in less pressure drop across the cells because the current collectors in this configuration is planar instead of porous It is important to consider that the viscosity increases due to collision between particles and against the wall.

This type of design has been applied in several battery, for example lithium–polysulfide (Li-PS), lithium–air (O_2), and metal ions in aqueous solvents. In the LI-PS battery, the overall pumping energy requirement is estimated to be lower for the dispersed nanocarbon in a flat current collector than conventional electrolyte through porous electrode. In this particular case, the addition of solid carbon particles facilitates more complete oxidation and reduction of the Li-PS chemistry. This permits to achieve higher total energy density in the electrolyte.

1.3.1.2 II: Flowing solid active materials with flowing carbon conducting

Both the active material particles and carbon are dispersed in the electrolyte flowing into the electrochemical cells, as shown in Figure 1.5.

The previous design is suitable for soluble or liquid electrochemically active materials, including those that form solid deposits, while this one is appropriate for systems where the electroactive material is a solid phase as particles.

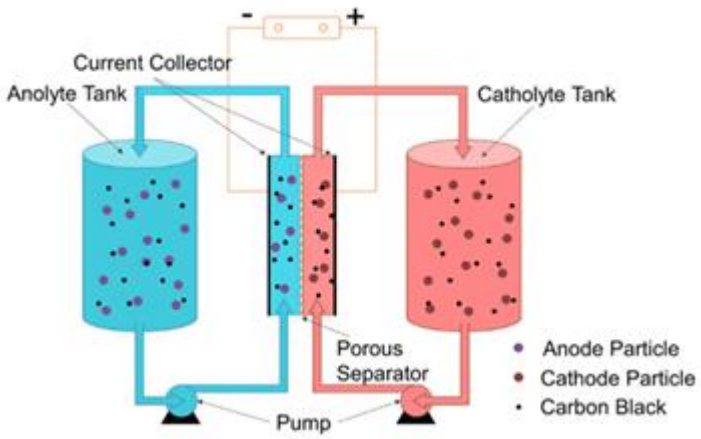

Figure 1.5 *Simplified representation of RFB with solid suspension of active material and carbon conductive network. (Qi and Koenig, 2017)*

The carbon or other conductive material needs to be smaller as possible (nanosize) to provide a large surface area with low loading of particles into the electrolyte.

In contrast with the previous design, the electrochemical reactions don't occur on the surface of carbon particles. Carbon works as a conducting network for electrons between the electroactive particles and the current collector, helping to improve the rate of electrochemical reactions. This idea has previously been reported as a semisolid flow cell (SSFC) by Duduta *et al.* (2011).

They have tested both slurry electrolyte coupled with Li metal anode and two slurry electrolytes coupled together. The main advantage of this design is the use of solid active material that provides high energy density to electrolyte. The capacity per volume of the battery increases thanks to the overcoming of solubility due to the use of solid particle suspension instead of soluble species.

Another interesting feature of this system is the possibility to separate the particles of the two slurries (cathodic and anodic) by size-exclusion. In principle, size-exclusion permits the use of porous separators, which are generally less expensive and give higher ionic conductivities than conventional ion-conducting membrane. This could be a key advantage if it is considered that one of the most expensive part in the conventional RFB is the membrane.

There are some challenges for researchers about this system.

The first drawback is the pumping energy lost due to the high viscosity. For example, the viscosity of the slurries reported by Duduta *et al.* (2011) is greater than 2 Pas at a shear rate of 10 s^{-1}. In addition, a high conductivity is needed to provide high power density; however, shunt currents are much more significant with a highly conductive carbon network, so it gives a loss of coulomb efficiency for a system as demonstrated by Xing *et al.* (2011).

Therefore, a trade-off between the power density and the coulomb efficiency is needed.

1.3.1.3 III: Flowing active material particles colliding on current collectors without carbon

A simplified representation of this design is reported in **Errore. L'origine riferimento non è stata trovata.**. The addition of carbon to the liquid medium results in a significant impact on the suspension viscosity that gives high pumping energy requirement. In the absence of carbon, three main characteristics change. The first is that viscosity decreases due to less particle loading; the second is that the mass and volume of components in the electrolyte that do not contribute to the cell energy is reduced;

third, without the percolating network, only particles in contact with the current collector (directly or indirectly through other particles) participate in electrochemical reactions at any given time.

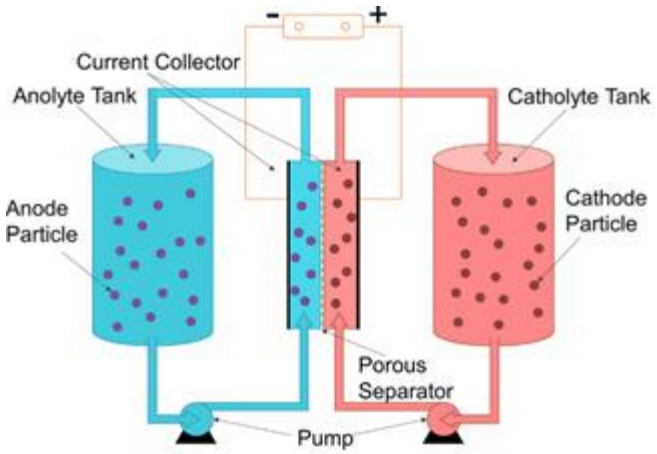

Figure 1.6 *Simplified representation of RFB based on solid active material suspension. (Qi and Koenig, 2017)*

This could lead to a loss in capacity utilization. In absence of flowing, the electrochemical activity become almost zero. The diffusion of ions and electrons during the collision between particles and current collector could limit the reaction rate. For this reason active materials with high electronic and ionic conductivity are particularly desired.

Great effort is needed to understand the material properties and flow profiles that maximize the energy efficiency. One possibility is to modify the surface of the active material particles to facilitate transport of electrons and ions and further reduce the suspension viscosity thanks to the repulsion between particles that decrease the frequency of collisions.

Another approach to improve the system design refers to an innovative flow channel which maximizes the active surface area per volume while minimizing pressure drops.

This configuration holds the advantage of using cheaper porous separators which works via size-exclusion.

1.3.1.4 IV: Targeted redox mediators as the power carriers with static solid active materials providing energy storage

The last design segment that is identified as “soluble redox mediators for power with solid active materials within tanks for energy”. In this case, the higher energy density of solid material is exploited immobilizing it in the tank as illustrated in Figure 1.7

A liquid electrolyte with soluble redox mediators flows cycling through the porous material in the tank and in the cell. For each compartment (cathodic and anodic) at least two redox reactions occur: one in the tank, between the immobilized solid material and the redox mediators, and another in the electrochemical cell at the electrode surface, as usual between electrode and soluble redox mediator. About the cathodic compartment, the mediator is oxidized in contact with the solid material in the tank and then it is reduced in the electrochemical cell as usual and so on. Vice versa in the case of anodic section.

In this configuration, the increased energy density by adding more material in the tank does not change the electrolyte viscosity, helping to keep down the pressure drop.

However, it should be considered that the electrolyte flows multiple times through both porous structure of tank (high energy active material) and electrochemical cell (porous electrode). This fact could give high total energy requirement for pumping.

The size exclusion benefit of separator is not applicable in this design because the redox active mediators are dissolved in the electrolyte and the solid material is immobilized.

Therefore, ion conductive membranes compatible with redox mediators are needed, and this is often the more expensive component of the battery.

The major application of this design is reported by Wei *et al.* (2015), which developed a full cell demonstration where $LiFePO_4$ (LFP) and $LiTi_5O_{12}$ are used as the cathode and anode solid energy storage materials, respectively. There are multiple mediators to exploit more reaction as possible, increasing the capacity and energy density of the system.

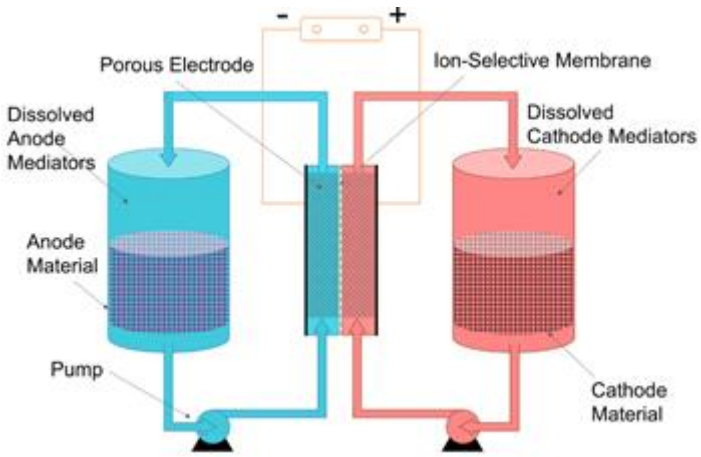

Figure 1.7 *Simplified representation of target redox flow battery with static active solid in the tank. Electrolyte is liquid. (Qi and Koenig, 2017)*

1.3.2 Active Material

In batteries, the active material stores the chemical energy and participate in redox reactions. Active material provides to the theoretical potential and capability of the battery.
The active materials are evaluated on several criteria: reduction potential, capacity, weight, conductivity (both ionic and electronic) and how flat is their plateau of discharging.
Obviously, the right interaction with liquid medium and other parts of cell are fundamental for the properly work of RFBs.
There are many types of active materials used in RFBs. Four main categories have been identified: 1) transition metal active materials, 2) organic redox species, 3) lithium intercalated materials and 4) sodium ion active materials.

1.3.2.1 Transition metal active materials

The single-element dissolved in aqueous electrolytes was the first type of active material used. The most common are transition metal ions (e.g., Fe, V) and halogens (e.g., Br, Cl) reported in Perry and Weber (2016). Some of the well-developed redox couple systems are soluble metal-bromine, iron-vanadium, iron-chromium and all-vanadium.
The main limit of the aqueous electrolyte is the voltage window, that it cannot exceed 1.23V. Over this value, electrolysis of water stars with evolution of H_2 and O_2.
The main challenges of this active materials are the low energy density due to limited solubility, narrow potential window and the efficiency of crossover through the membrane.
The membrane has to perform high cation-selective permittivity, low conductive resistance and acceptable cost. Nowadays, the all-vanadium RFB has reached the best performance. It works exploiting all four oxidation states of vanadium (V^{2+}, V^{3+}, V^{4+}, V^{5+}) two for each compartment, as it is shown in Figure 1.8. In this way, the reducing of cell life caused by the crossover of the

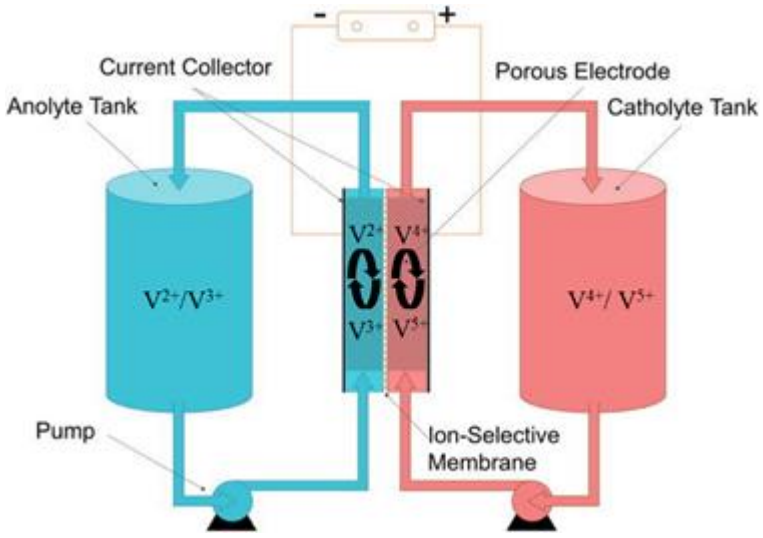

Figure 1.8 *Simplified representation of conventional vanadium redox flow battery (VRFB)*

species through the membrane is limited by self-nature of the species. The unique consequence of a crossover is the direct reaction between redox species, which decreases the capability of the battery in a specific charge or discharge cycle.

All-Vanadium batteries have been documented by Winsberg *et al.* (2017) with energy density equal to 25 Wh L^{-1} that is a good value for large stationary storage but not enough for the transportation industry and portable devices that they require at least 250 Wh L^{-1}(like Li ion battery). The transition metal compounds have been used with solid particles in RFB described in the §1.3.1.1.

For example, a Zn-Cu active solid suspension battery has been proposed in Mubeen *et al.* (2016). The electrochemical redox reaction is reported in (1.1

$$Cu_{solid} + Zn^{2+}_{solution} \leftrightarrow Cu^{2+}_{solution} + Zn_{solid} \quad (1.1)$$

At the beginning, Zn is deposited on carbon particles and Cu^{2+} is dissolved in the electrolyte. During discharge, Zn dissolves, and Cu is deposited onto the surface of solid particles.

Voltage of 0.97V is achieved with an energy efficiency of 70% at a constant current density of 5 $mAcm^{-2}$. The proposed approach provides the possibility to expand capacity significantly.

1.3.2.2 Organic active materials, including polymers

Organic molecules provide a wide range of design flexibility and desirable attributes regarding redox potentials, windows stability, solubility and other physicochemical properties. They could be used with both organic and aqueous solution and, in some cases, they present advantages by reducing costs and the toxicity risk.

In particular, organic active materials are generally soluble in organic solvents that have wider window stability. Also in this type of active materials, one of the main challenge is the crossover of organic molecules through the separator. Development of new membranes it could be difficult and very expensive.

Montoto *et al.* (2016) proposed to use redox active colloids (RAC) as the active material the crossover. Solid xPVBC particles are synthesized through emulsion polymerization as support for redox couples. The redox couples are grafted onto xPVBC through ion exchange by replacing -Cl on xPVBC. The final RAC particles are made. The functionalization efficiency was nearly 100%. RACs had good morphology and chemical stability during charge/discharge and minimal membrane crossover.

Some challenges reported by Montoto *et al*. (2016) have to be solved. Assuming a high concentration of 40 wt. % and an average discharge voltage of 0.85 V, the energy density should be approximately 12.5 Wh L^{-1}, absolutely not enough for the transportation industry. Support material with low density and low molecular weight has to be applied to increase the energy density. A key issue is the high viscosity at high RAC loadings. A 40%wt RAC shows more than 10 Pa s at 100 s^{1} shear rate. The value of viscosity is significantly higher than many other suspension-based systems.

Overall, these grafted redox couples on inert backbone particles are promising approaches to overcome the solubility limitation. More innovations on material selection and engineering are expected to increase the performance significantly.

1.3.2.3 Lithium-ion intercalated materials

The main propriety that differentiates this type of materials is the capability to intercalate atoms. The intercalation is a reversible reaction where atoms/molecules is putted into the layered structure of material. The main advantages of intercalation are the high reversibility of reaction and the flexibility. The last one feature derives from the possible combinations between materials that host and intercalated atoms.

To increase the energy density, Li atom is the widely used due to its low molecular weight.

This type of active materials is generally solid. For this reason, it cannot be used in RFB-design I described in §1.3.1.1. The knowledge of this material comes mainly from the development of Li-ion battery that is the best technology for small and medium size batteries. There is a big effort in researcher community about this topic and there are lots of intercalated materials with different reduction potential and capacity. All these materials could be paired, making a new electrochemical cell because all those intercalate/deintercalated Li.

These materials could be used in RFB with design flow II, III and IV , described in §1.3.1, because they are all solid active materials.

In particular, $LiCoO_2$ (LCO) is one of the most widely used Li-ion cathode material. It has a layered structure and well known electrochemical properties. It has been applied in RFB-design II and III , described in §1.3.1.2 and §1.3.1.3 respectively.

A suspension of 22.4 %vol. LCO with 0.7%vol. KB shows a reversible capacity of 127 mAh g^{-1} LCO, close to the theoretical capacity equal to 137 mAh g^{-1}. LCO has a discharge voltage of 4.0V versus Li/Li^+ as it can be noticed in Figure 1.9.

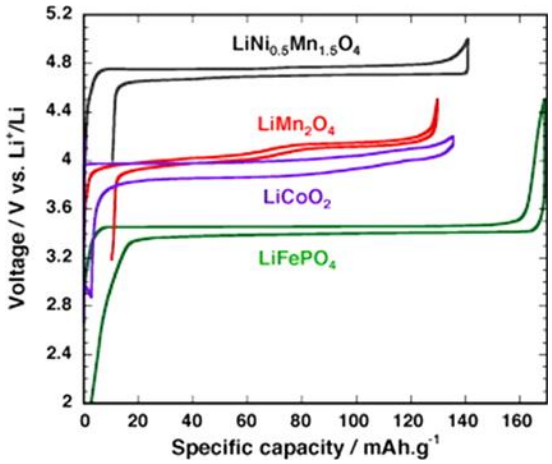

Figure 1.9 *Graph of Voltage vs Capacity of charge and discharge process of different Li ion cathode material paired with Li metal anode. (Qi and Koenig,2017).*

LCO has relatively high electronic and ionic conductivity. Nevertheless, some limitations need to be taken into account when LCO is used in RFBs. First issue is the environmental impact of Co, so the recycling of Co from the battery is fundamental and it should be easier. Second, the cost of Co is relatively high because of its relatively low earth abundance.

Other interesting material is $LiMn_{1.5}Ni_{0.5}O_4$ (LMNO) that is a spinel-phase material with a high voltage of 4.7V versus Li/Li^+ (shown in Figure 1.9) and high theoretical capacity of 146 mAh g^{-1}, suggesting a theoretical energy density of 686Wh kg^{-1} as reported by Liu at all (2010).

In addition, Ni and Mn are both less expensive than Co. LMNO has been used in a RFB-design II (flowing solid active material plus carbon network) by Duduta *et al.*(2011). In this article a suspension of 20 vol.% LMNO and 2.5 vol. % carbon was cycled as a half cell achieving close to theoretical voltage and high capacity. Long-term cycle life is the main challenge for this material due to the high potential of LMNO which exceed the windows stability of lots of electrolyte. This aspect is investigated by Liu *et al.* (2010).

$LiMn_2O_4$ (LMO) is a material that has a spinel structure and shows a plateau in potentiometric curve at 4.0V versus Li/ Li^+ and a theoretical capacity of 148 mAh g^{-1} (shown in Figure 1.9) as reported by Robinson and Koenig (2015). It has a lower cost and is more environmental friendly than previous materials, but the dissolution of manganese in the electrolyte, investigated by Doi *et al.* (2008), causes a capacity loss. The ionic and electronic conductivities are also relatively low.

$LiFePO_4$ (LFP) is a cathode material with a plateau in potentiometric curve at 3.5V versus Li/Li^+ and theoretical capacity of 169 mAh g^{-1} (shown in Figure 1.9), as reported by Zhang (2011). LFP has cost, environmental, and safety advantages. It also has a flat discharge voltage profile. The flat profile can be beneficial for design based on stochastic particles collision as RFB-design II and III. LFP was demonstrated as a cathode material for RFBs in both design II by Li *et al.* (2013) and design IV by Wei *et al.* (2015). The main challenge is the high viscosity caused by collision between particles and against the wall. Furthermore, the effects of particle size and morphology are not well studied for RFBs.

$Li_4Ti_5O_{12}$ (LTO) is an anode material and it has been demonstrated in RFB-design II and IV. It has high theoretical capacity of 175 mAh g^{-1} and Li insertion voltage of 1.55V versus Li/Li^+. The discharge curve is very flat, providing a stable voltage output. Ohzuku *et al.* (1995) has noticed that LTO has good particle morphology and crystal stabilities. In addition, LTO has excellent ionic and electronic conductivities.

Anatase TiO_2 is another anode material with an average potential of 1.8V versus Li/Li^+ and a theoretical capacity of 330 mAh g^{-1} and it has been reported in RFBs in several types of design. Liu *et al.* (2016) reported that TiO_2 has cost, environmental, and safety advantages and a high ionic conductivity, but the electronic conductivity and rate capability are low respect to other anode materials.

Other materials like Li ($Ni_xMn_yCo_z$)O_2 (with varying compositions of x, y, and z) and vanadium oxides are also under active research.

1.3.2.4 Sodium-ion active materials

Na-ion battery materials have attracted attention because it is more earth abundant and cheaper than Li and, in some cases, allows for alternative material choices in the battery cell.

Ventosa *et al.* (2014) reported a nonaqueous RFB using P2-type $Na_xNi_{0.22}Co_{0.11}Mn_{0.66}O_2$ (NaNCM) and $NaTi_2(PO_4)^3$ (NaTP) as the cathode and anode active materials, respectively. NaTP operates at a flat potential of 2.1V versus Na/Na^+ and has a capacity of 125 mAh g^{-1} NaTP. P2-type NaNCM was demonstrated to have a capacity of 130 mAh g^{-1} with a range of potential plateaus between 2.1-4.3 V versus Na/ Na^+.

A reversible energy density of 9Wh L^{-1} is demonstrated, although it is suggested that a value of around 150Wh L^{-1} would be achievable. The main challenges in this system are high overpotential and low gravimetric capacity relative to high energy spent to pump the viscous suspension.

Na-ion materials provide an alternate route to using solid intercalating particles in RFB systems.

1.3.3 Flow and Agitation Methods

The flowing of fluid from tank to cell and vice versa in RFBs is provided by an amount of energy spent. This energy is usually released by pump, but there are other methods to move the fluid.

In general, the fluid could be moved in continuous, intermitted or batch stirring mode.

Different kind of forces that can move the fluid in RFBs are reported in the following paragraphs.

1.3.3.1 Continuous pumping, intermittent pumping, and batch stirring

The conventional operation mode is the continuous pumping, where the fluid circulates between tank and electrochemical cell. It is the conventional one for soluble transition metal RFBs because:

1) the energy density of the fluids is limited and continuous charged electrolyte in the cell is required to guarantee a stable power output;

2) the fluids that have been charged/discharged in the electrochemical reaction cells are mixed with the charged electrolyte in the tank, allowing a gradual change in redox active species concentration;

3) the fluid viscosities are typically low, making continuous pumping easy to implement.

In the case where the solid active particles are in suspension and the viscosity increases very quickly a different operation mode could be more useful.

In particular, the increasing of energy density and viscosity could suggest an intermitted flow mode. During the intermitted flow, an amount of charged electrolyte is putted in the cell and the discharged particles are putted out. The charged particles stay in cell until they are dead and then the cycle restart. This approach permits to save energy as Duduta *et al.* (2011) demonstrated.

Using RFB-design II (§1.3.1.2) a pumping energy loss of 44.6% is estimated in continuous mode; this value decreases to 0.6% in intermitted flow. It is important to know that this estimation does not take into account about initial viscosity and, generally, viscosity of solid suspension is very highat low shear rate. In this operation mode the conductivity has to be high because the fluid is not stirred. The presence of carbon or other high conductive medium can rise up this propriety. For these reasons RFB-design I and II can be apply with intermitted operation mode

In RFB-design III (§1.3.1.3) the frequency of collision between particles and current collector is fundamental for the performances of electrochemical cell. For this reason, the intermitted flow is not suitable.

An alternative is the batch stirring mode, analysed by Qi and Koenig (2016). In this operation mode an amount of particles is introduced in the electrochemical cell and continuously stirred during the discharge to ensure high frequency of collision achieving good cell performance. In this case there is an additional energy requirement due to the stirring. The mixed environment facilitates the ion diffusion thanks to convection transport.

A disadvantage of these alternative designs is that they require four tanks, two for each compartment: two for charged solutions (anodic and cathodic) and two for discharged solutions (anodic and cathodic). In addition, a switch system has to be implemented to guarantee a stable output although the discontinuous mode. This means that we're adding system complexity, which results in a corresponding increase of system size and costs.

1.3.3.2 Other driving forces for electrolyte

Other innovative approaches have been reported in literature for flow cells.

A gravity-induced flow cell design (GIFcell), shown in Figure 1.10, was proposed by Chen *et al.* (2016).

The movement of fluid between cell and tank is driven by the force of gravity. The cell is flipped mechanically when all electrolyte is passed through the current collector. In the case that electrolyte is completely discharged at the first passage, the second one is obviously useless and the cell will be not flipped. The energy input to mechanically flip the cell is expected to be significantly smaller than energy spent to pump the viscous electrolyte.

The number of flip depends on the flow rate, which is controlled by channel dimension, surface properties, tilt angle of the channels, and cycling rates. All these parameters have to be

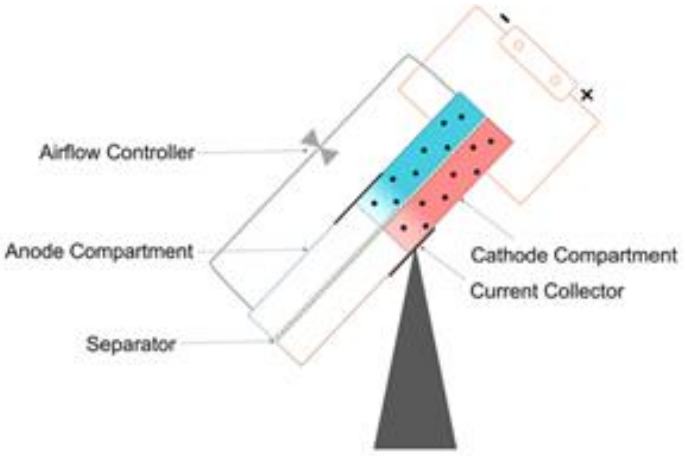

Figure 1.10 *Illustration of gravity induced flow cell design*

optimized to minimize the energy loss. The mixing of the suspension is provided by the structure of the current collector (or static electrode).

In general, the gravity force could be used as a complementary to pumping. Demonstration of this concept is reported in Chen *et al.* (2016) applied to Li-PS chemistry. In this article the mechanical energy for flipping the cell 25 times (required to discharge battery) is calculated to be only 0.01% of the energy stored in the cell.

The magnetic force acting on particles is another useful force that could be used to drive fluid movement in RFBs. γ-Fe_2O_3 nanoparticles suspension is well-known as ferrofluids. It has been used as additives to provide transport advantages under magnetic field as reported by Sen *et al* (2015b).

Instead, Li *et al.* (2015) reported a Li-PS battery with added γ-Fe_2O_3 particles in a conventional static cell geometry and used applied magnetic fields to improve electrochemical properties. The performance is improved by concentrating the active material near the current collector. In this suspension, γ-Fe_2O_3 nanoparticles absorb PS on the surface and they are concentrated near the current collector due to magnetic field, providing benefits with regard to mitigating PS shuttling and increasing the achievable discharge current densities.

The magnetic particles under magnetic field can drive the fluid rather than pumps as demonstrated by Li *et al.* (2015). The advantages of flowing the fluid with magnetic field result in a more precise control of the flow rate and direction, in a simpler system and the possibility to save energy. The main limit is the requirement of ferro-magnetic particles. Energy density decreases due to the presence of these particles. They add volume and weight, but they do not contribute to increase energy density. Moreover, they could interact negatively with the redox reaction that occurs in the cell.

Chapter 2

Nanofluids Development

To test the feasibility of the technology, cathodic and anodic nanofluids have been developed. In this chapter, the criteria and methodology adopted to design electrolyte suspensions are presented. Selected nanoparticles have been treated, by using a coating process proposed in literature, and suspended in a suitable solvent. The biphasic mixtures were then added with selected electrolyte to increase their conductivity.

2.1 Nanofluids in literature

In this paragraph the nanofluids, chosen among those available in literature because fit for purpose, are presented in details. The selection of these electrolytes is mainly based on energy density and viscosity, which are the more important performance parameters for transport industry.

The study doesn't explore nanofluids (Katsoudas *et al*.(2014)) whose synthesis process is patent protected.

2.1.1 TiO_2 nanofluids

This nanofluid has been investigated because it is a very good Li intercalated anodic material. Sen *at el.* (2015) developed a very efficient surface treatment on the nanoparticles to decrease the viscosity of the aqueous suspension.

The surface treatment prevents the aggregation of particles and reduce the frequency of collisions between them, decreasing the viscosity.

After treatment, the nanoparticles were suspended in ethylenglycol/water solution which show a typical shear-thinning behaviour. Results are shown in Figure 2.1a.

As it can be noticed, a viscosity around 4mPas at 50%wt of particle loading, at room temperature, can be achieved. Modified particles have only 3%wt of the material on the surface which guarantees a stable suspension for 2 weeks, at least.

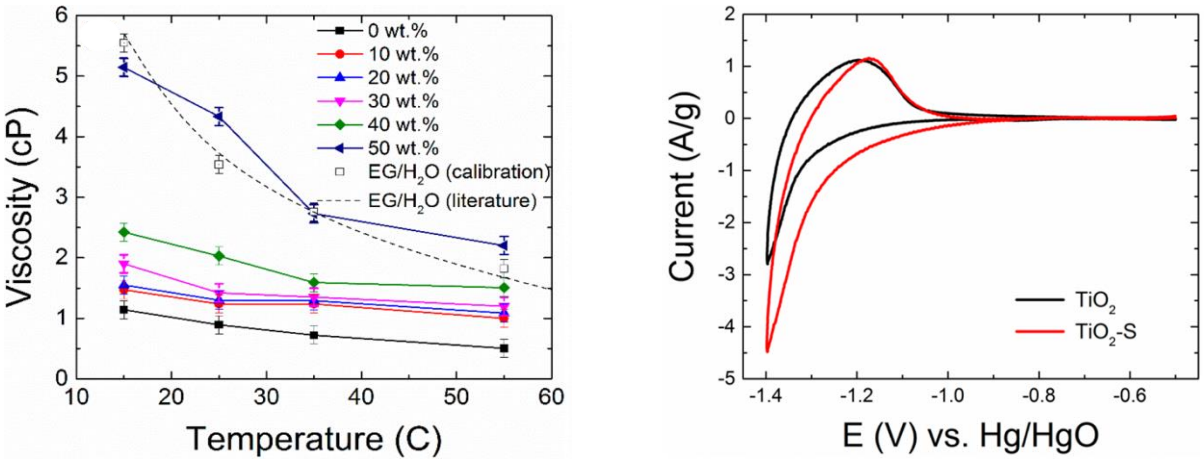

(a) (b)

Figure 2.1 *(a) value of viscosity at different loading and different temperature of a nanofluids of TiO2 in water -based solution. (b) cycle voltammetry of a solid castled electrode of TiO2 in solution of 4M KOH/1.5M LiOH at scan rate of 5mV/s.*

The electrochemical performance has been evaluated through cycle voltammetry (CV) that has been carried out using both pristine and treated nanoparticles. As it can be noticed in Figure 2.1b, the reduction standard potential is around -1.2V vs Hg/HgO. The stationary current can't be exactly estimated, but its value is not high. The increasing of the current at -1.3V vs Hg/HgO in the same figure is caused by the evolution of H_2. The current is higher for the treated particles than pristine one due to the improved concentration of H^+ on the particle surfaces.

Results of this study show a decrease of 22% in electrochemical activity of modified particles due to the presence of the surface coating.

No information about the energy density of the nanofluids is reported but the pristine material has generally a high capacity.

Therefore, the interesting feature of this approach is the huge improvement in viscosity performance, retaining good electrochemical performance.

2.1.2 *$Li_4Ti_5O_{12}$ nanofluid (LTO)*

LTO is very good Li-ion anode material and for this reason it has been studied in nanofluid form by Qi and Koenig (2016).

Both coin solid cell and flowing cell with nanofluid (20%vol of solid) were tested to investigate the effect of the conductivity between the particles. The tests were carried out in a particular cell shown in Figure 2.3.

The tests on coin cell show a capacity of 110mAh, reduction potential equal to 1.5V vs Li/Li^+ and very flat discharge curve. These performances are typical of conventional LTO half-cell.

The conductivity of the LTO material increases with lithiation until 100 S cm^{-1}.

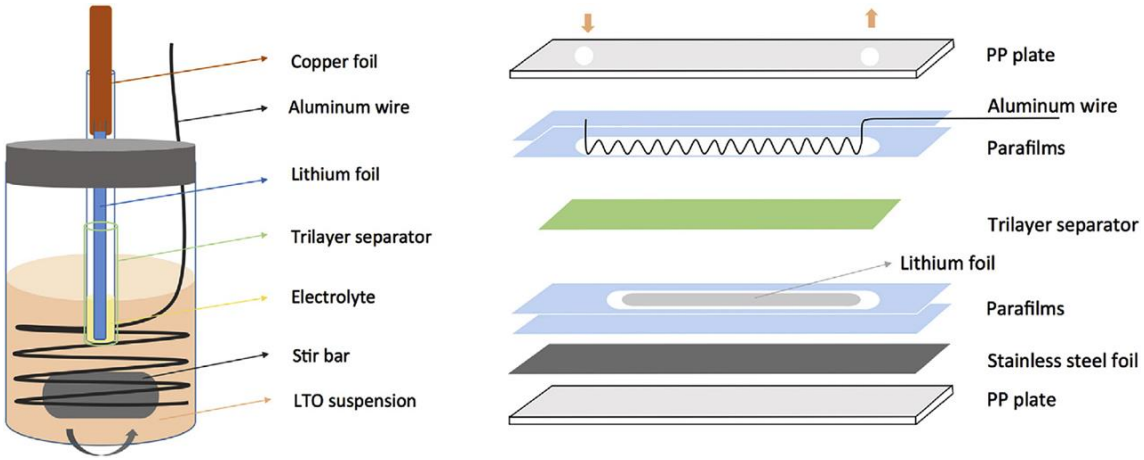

Figure 2.3 *Cartoon schematic of cell configurations: (a) a vial cell with the aluminum wire in the LTO suspension as the cathode current collector and the lithium foil in the glass tube as the anode; (b) a flow cell with an aluminum wire current collector in the channel containing the LTO suspension and lithium foil attached on the stainless-steel foil as the anode. (Qi and Koenig, 2016)*

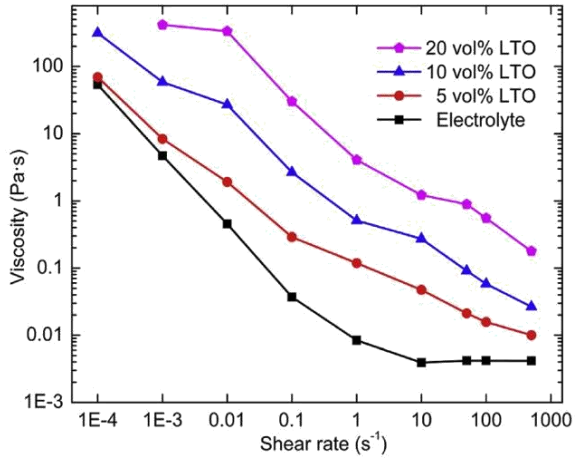

Figure 2.2 *The viscosity as a function of shear rate for the particle-free electrolyte (1.2 M LiPF6 in EC/EMC ¼ 3:7 solvents, black squares) and the electrolyte laden with 5 , 10 and 20 vol% LTO.(Qi and Koenig,2016)*

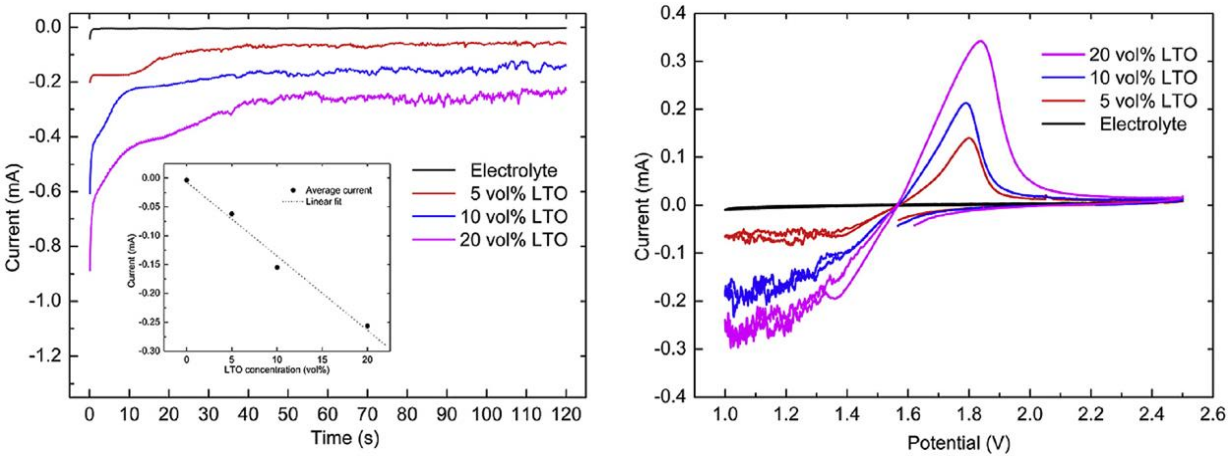

(a) (b)

Figure 2.4 *(a) Chronoamperometry (CA) profiles at 1.2 V and (b) cyclic voltammetry (CV) scans at the rate of 5 mV s-1 for the particle-free electrolyte, potential is referred to Li/Li+ and the electrolyte laden with 5 (red), 10 (blue), and 20 (purple) vol% LTO as measured in the vial cell. (Qi and Koenig,2016)*

Figure 2.2 summarizes the rheological behaviour of the particle-free electrolyte (by 1.2M LiPF6 in EC/EMC=3:7) and the electrolyte with different particle loading, measured at room temperature. The viscosity changes multiple orders of magnitude over the share rate investigated, decreasing with the shear rate increasing. It rises with LTO concentration, being significantly higher than particle-free electrolyte at 20%vol. This behaviour is consistent with the shear-thinning behaviour of a solid suspension.

The electrochemical performance, for increasing particle loadings in electrolyte, was evaluated through chronoamperometry (CA) (Figure 2.4a) and cycle voltammetry of nanofluid (Figure 2.4b). The free-particle electrolyte was used as a control. At the beginning of the CA experiments, the current is very high due to accumulation of particles around the collector; then it decreases by reaching a steady-state value of a few tenth of mA.

The fluctuations are due to the discrete collisions of particles with the current collector.

The CV curves confirm the dependence of the measured current on LTO concentration. It can be noticed that the reduction peak is not present, while there are significant oxidation peaks, even if only a very small fraction of the LTO particles (which initially should all be in the oxidized state) have been reduced. The estimated fraction of the LTO material in the suspension that it has been reduced is less than 0.01% of the total electrochemical capacity within the solid dispersion.

These results indicate that the kinetic is very slow or in that specific system is present some limitation. CA test evidences that the limit of the stable current is approximately 0.10 mA for 5%vol nanofluid, although this value is strongly affected by the stirring level and by the shape of current collector.

No specific investigation on this behaviour are reported in literature.

All these results indicate that Both rheological and electrochemical properties of LTO suspension should be improved to get the required characteristics, even if the proprieties of pristine material are very good.

2.1.3 *LiFePO4 (LFP)*

This compound is a very good Li-ion intercalated material with high theoretical voltage and capacity; for this reason it is investigated.

A mixture of LFP with carbon and polyvinyl pyrrolidone (PVP) has been proposed by Wei *et al*. (2015) as solid material for the nanofluid.

The role of carbon is to increase the conductivity between the particles, while PVP is added for reducing the viscosity of the nanofluid.

The system shows an energy density of 93 Wh L^{-1}, but the viscosity is around 200 Pas with initial stress of 660Pa (Figure 2.5).

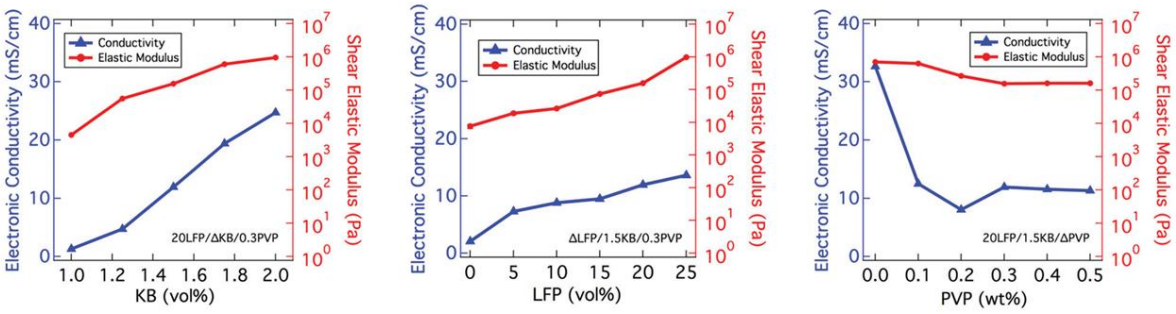

(a) (b) (c)

Figure 2.6 *a) Plots of shear elastic modulus and electronic conductivity as a function of varying KB (at 20 vol% LFP, 0.3 wt% PVP), b) LFP (at 1.5 vol% KB, 0.3 wt% PVP), and c) PVP (at 20 vol% LFP, 1.5 vol% KB) contents showing positive correlation between the two properties. (Wei et al.,2015)*

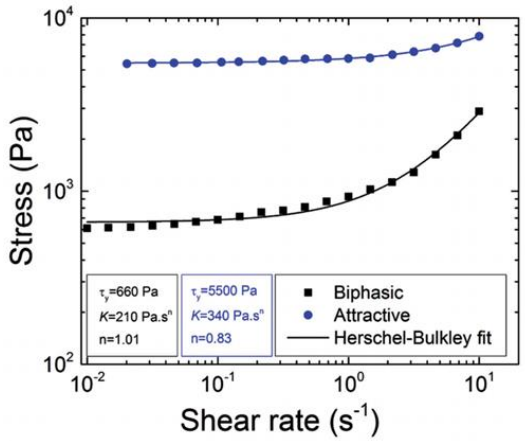

Figure 2.5 *Log–log plot of shear stress as a function of shear rate for biphasic (0.3 wt% PVP) and purely attractive (0 wt% PVP) electrode suspensions composed of 20 vol% LFP and 1.25 vol% KB. (Wei et al.,2015)*

Studies about the influence of the quantity of the component have been carried out and results are reported in Figure 2.6. As it can be noticed in Figure 2.5c, the percentage of PVP doesn't affect the electronic conductivity over 0.3%wt.
Therefore, , an increasing of quantity of this component in the suspension could be considered in order to decrease the suspension viscosity.
A suspension 20LFP/1.5KB/0.3PVP presents a coulomb efficiency equal to 99% and a specific capacity of 129 $mAhg^{-1}$ at C8 that remains almost constant during the cycles. The reduction potential is equal around 3.3V vs Li/Li^{+}.
The energy density is significantly lower than conventional Li-ion battery, but improvement in electrochemical performance could be obtained increasing the particle loading. The major obstacle to the application of this nanofluid is its viscosity. Performing flow cell in intermittent flow mode, the energy loss in pumping could be reduced. However, further solutions to decrease the viscosity should be investigated.

2.1.4 *Conclusion*

Table 2.1 resumes the main characteristics of nanofluids found in literature.

Table 2.1 *Summary table of main characteristics of electroactive nanofluids available in literature*

Material	E^0[V] (vsLi/Li+)	Capacity/energy density	Viscosity [mPas]	Main Limit
TiO_2	1.9	Estimated high	4 (50%wt loading)	Aqueous solution
LFP	3.3	93Wh/L	$2 \cdot 10^5$	High viscosity
LTO	1.55	Not Estimated-low conversion	$10\text{-}10^5$ (high shear rate)	Expensive investigation needed

As it can be noticed, only TiO_2 show appealing features to be used in transport industry, even if its energy density in aqueous solution could be low. LFP has a huge viscosity, while LTO needs further investigation for improving its proprieties.
Then, TiO_2 was selected for the anode nanofluid. In order to improve its performance, a surface treatment has been considered.
Not having found in literature a satisfactory solution for the cathode nanofluid, a new suspension has been developed.

2.2 Nanofluids Developed

The design of nanofluid is based on Li-ion compounds for both the anode and cathode compartment. To optimize the battery performance, suspensions must have high energy density and low-dissipation flow. High active material content in nanofluid ensures high energy density; however as the solid loading increases, dramatic changes in rheological properties of the suspension occur, which inhibit flow. Therefore, attention was focused on the possibility to reduce interaction within the active particles and between the medium and the particles using tailored surface treatments, which don't inhibit electrochemical activity.

2.2.1 *Surface Treatment*

Sen *at el.* (2015) proposed a surface treatment based on condensation reaction between the hydroxide of TiO_2 in the surface and 3-(trihydroxy silyl)-1-propanesulfanic acid.
As shown in Figure 2.7, around the particle, in alkaline condition, there is a negative charge

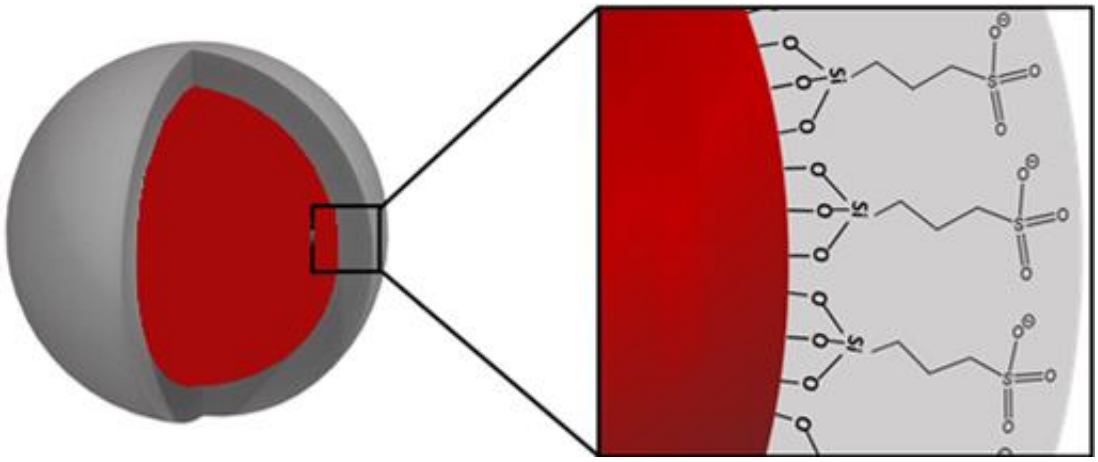

Figure 2.7 *Schematic representation of the surface treatment*

layer due to the deprotonation of -OH group. As the sulfonic group is a strong acid, it easily gives up its proton to a base.
The same process was successfully used by Sen *et al.* (2017) for treating Fe_2O_3 particles.
This analysis highlights that the treatment is applicable at active materials having -OH group at the surface of the nanoparticle; moreover the, sulfonic group permits the passage of positive ions, helping the transfer of Li^+ between solid particle and bulk.
In this thesis, the coating process has been used to treat TiO_2 nanoparticles for the anode suspension. Aiming to treat the active material of cathode electrolyte in the same way, the choice of nanoparticle was oriented toward compounds having –OH group on the surface.

2.2.2 *Active Material*

Selection of the cathodic active material has been done keeping in mind that it had to be a metal oxide (or some material with -OH group in the surface) and it had to intercalate Li ion in its own structure.

The criteria to choose material are: right reduction potential to permit the use of aqueous solution (no more than 3.1V vs Li/Li^+), high capacity ($mAhg^{-1}$), high conductivity and the reliability of the material to have well known pristine proprieties.

In this flow design the conductivity of material is particularly important.

Figure 2.8 shows the range of capacity and potential of several cathodic metal oxide.

It can be noticed that only MnO_2 and V_2O_5 show an acceptable potential that permits the use of aqueous solution (ΔV=1.23V). The max potential acceptable is 3.1V vs Li/Li^+ because the potential of TiO_2 is 1.9V vs Li/Li^+.

The commercial nanoparticles of MnO_2 show a very limit capacity around 30mAh g^{-1} (Huang *et al.* (2010)). Tang *et al.* (2003) developed MnO_2 nanoparticles showing high capacity, but this compound has a carbon layer which does not permit to apply the surface treatment.

With reference to V_2O_5, there are no commercial availability of nanoparticles and no data in literature that permit to make nanoparticles having good electrochemical characteristics.

The aqueous solution cannot be applied because there are any material within the windows stability of water. More stable solvent is needed.

Therefore, the possibility to choose material with potential higher than 3.1V vs Li/Li^+ has been considered.

In Figure 2.8 there are only few reliable materials: $LiCoO_2$, $LiMnO_2$ and $LiNi_{0.5}Mn_{1.5}O_4$. Others materials are not well developed and their performance and stability are not well known.

$LiMn_2O_4$ has two plateau, the first at 4.2V and the second one around 3V vs Li/Li^+.

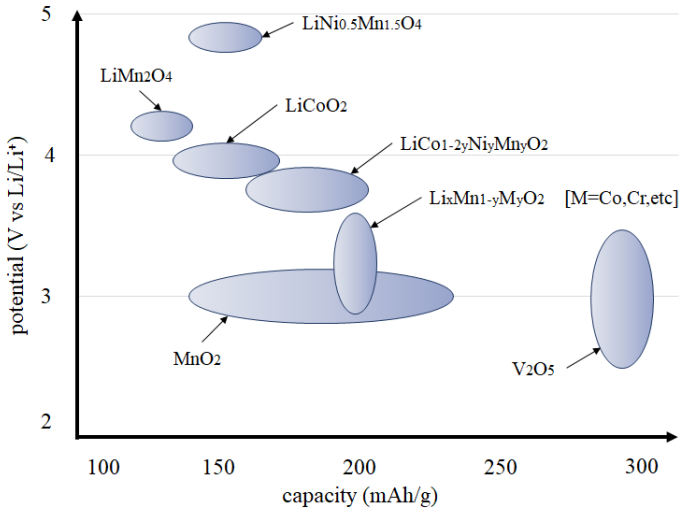

Figure 2.8 *Potential vs Capacity graph of some metal oxide cathodic material. (http://forschung-energiespeicher.info/en)*

This feature represents a limit in this type of design because all particles have to discharge the first plateau before to deliver the electrode corresponding to the second one. If some particles discharge electron at higher potential, current collector has a potential higher than particle, so there is not driving force. In addition, it presents a dissolution phenomenon of material in several solvent causing a quick decrease of capacity (Curtis *et al.*(2004)). Moreover, the conductivity of the material is not high. For all these reasons LMO it is not suitable for this application.

$LiCoO_2$ is widely used in modern Li-ion battery and it shows a high conductivity and stability. Different sizes of nanoparticle are viable in market.

$LiNi_{0.5}Mn_{1.5}O_4$ is less used than LCO but it has a higher potential reduction and the same capacity.

LNMO is less expensive than LCO but the high voltage can cause problems for the stability of the solvent.

Commercially, LMNO is easily viable in nanoparticle form and present better performance, so it has been chosen as active material.

2.2.3 *Solvent*

The liquid medium where the solid nanoparticles are suspended is composed by solvent and electrolyte. Due to the choice of active material, the aqueous medium cannot be applied.

To get the best performances, the solvent has been selected using the following criteria, sort by importance:

1. Windows stability from 1.5V to 5.0V vs Li/Li^+.
2. High donor number: it permits to deprotonate the sulfonic group and create the negative layer around nanoparticles.
3. Boiling and melting point which permit to work at liquid state.
4. High flash point and autoignition point: for safe reason they have to be enough higher than working temperature.
5. Cost.
6. Reliability: solvent widely used in similar application assure stability and good performance.
7. Low Viscosity: save energy in the pumping.
8. High conductivity of Li^+: rise the electrochemical performance. It increases mainly thanks to electrolyte.
9. High concentration of Li-ion soluble.
10. Low density: it means higher energy density of the electrochemical cell.

The selected solvents are resumed in Table2.2.

Table 2.2 *Table of nonaqueous solvent and some proprieties and features. The values are reported from "Electrochemistry in nonaqueous solution, Kosuke Izutsu,2008, chapter1". Other sources are specified. a= Handbook of organic solvent properties b=database of "Institute for occupational safety and health of the german accident insurance" (www.dguv.de/ifa/gestis/gestis-stoffdatenbank/) c= www.sigmaaldrich.com*

Solvent	**Donon Num.**	**Boiling-(Melting) point [°C]**	**Flash Point (autoignition point) [°C]**	**Viscosity [mPas]**	**Ionic Conductivity [Scm^{-1}]**	**Density [KgL^{-1}]**	**Cost [€/L]**
Water	33	100(0)		0.89	$6\cdot10^{-8}$	0.98	0
Acetone	17	56.1(-94.7)	18(465)[a]	0.3	$5\cdot10^{-9}$	0.78	50
Propionitrile	16	97.4(-92.8)	2(510)[b]	0.39	$8\cdot10^{-8}$	0.77	80
Formamide	24	210.5(2.5)	152[b]	3.3	$<2\cdot10^{-7}$	1.1292	160
N-Methylformamide (NMF)	49	180.9(-3.8)	116(490)[b]	1.65	$8\cdot10^{-7}$	0.99	130
N-Dimethylformamide (DMF)	26	153.0(-60.4)	58(440)[b]	0.80	$6\cdot10^{-8}$	0.94	120
N-Methylacetamide (NMA)	n.d.	206 (30.5)	116(490)	3.65	$2\cdot10^{-7}$	0.95	50
Pyridine	33	115.3(-41.6)	20(522)[a]	0.88	$4\cdot10^{-8}$	1	200
1,1,3,3-Tetramethylurea (TMU)	29	175.2(-1.2)	75[b]	1.40	$<6\cdot10^{-8}$	0.95	400
N,N-Dimethylacetamide (DMA)	27	166.1(-20)	58(440)[b]	0.93	10^{-7}	0.9369	170

Acetonitrile	14	81.6(-43.8)	6(524)[a]	0.34	$6 \cdot 10^{-10}$	0.77	120
Ethylene Carbonate	16.4	248.2(36.4)	143(450)[b]	1.90	$5 \cdot 10^{-8}$	1.33	50
Propylene Carbonate	15.1	241.7(-54.5)	135(430)[b]	2.53	$1 \cdot 10^{-8}$	1.2	100
Diethylene Carbonate	16	126(-43)	25(445)[b]	0.83	/	0.97	400

Water is reported as reference because it is the solvent used by Sen *et al.* (2015) in TiO_2-based anode suspension. In particular, an aqueous solution with pH equal to 12 makes Li stable, as explain in Casellato *et al.*(2006).

Donor number of the water is equal to 33 and it increases at high pH. It is not possible to determine the minimum donor number needed to deprotonate the entire layer of treated particle. Sulfonic group has good dissociation constant. This feature suggests a low donor number needed. Electrolyte in the solvent influences the donor number.

Boiling and melting point have been taken into account to evaluate the stability of medium at working temperature, that is slightly higher than ambient due to joule effect.

Solvents with melting point higher than -10°C and boiling point less than 90°C have been discharged. Boiling point lower than 90°C, in fact, means a high volatility at working temperature.

Flash point and autoignition point are fundamental parameters in the transport industry. A flash point minimum 80°C has been required. The value reported is referred to closed cup. The choice of the minimum value of flash point or boiling and melting point is arbitrary.

Considering these requirements, propylene carbonate seems to be the best choice. Moreover, propylene carbonate it is also used in several Li ion battery application as solvent.

It doesn't have a low viscosity, but the particle loading is the factor that mostly influence rheological properties of the nanofluids.

Conductivity, density and solubility of Li are on average.

The electrolyte chosen is the $LiClO_4$ because it is widely used in literature on Li-ion battery.

2.3 Conclusion

No enough performant nanofluids has been found in literature. To test the feasibility of this technology it has been developed two nanofluids (anodic and cathodic). The anodic nanofluid is based on TiO_2 nanoparticles with surface treatment proposed by Sen *et al.*(2015) in a organic liquid medium. The cathodic one is composed by LMNO nanoparticles treated in the same way and suspended in the same organic liquid medium. The best liquid is propylene carbonate (PC) with $LiClO_4$. It guarantees a wide windows stability and high donor number.
The best liquid medium is composed by propylene carbonate (PC) and ethylene carbonate (EC) in 7:3 wt ratio which it is stable in the working electrochemical windows. $LiClO_4$ is used as electrolyte to increase the conductivity and to provide a lithium ion.

Chapter 3

Materials and Methods

In this chapter the materials and methods applied to prepare and analyse the samples have been described. The chapter is divided in four paragraphs: nanoparticle treatment, cyclovoltammetry, chronoamperometry and viscosity measurement. The motivation that leads to perform these analyses will be discussed in the chapter 4.

3.1 Nanoparticles preparation

Commercially available nanoparticles of $LiMn_{1.5}Ni_{0.5}O_4$ (Sigma Aldrich <200nm) and TiO_2 (anatase, Li-ion technology, 10-25nm) were used in this work. They were treated by a reaction of condensation, explained in §2.2.1. The surface modification process was carried out in aqueous solution and the resulting particles were transferred in propylene carbonate solution. There are some differences between the production protocols of the two materials.

3.1.1 TiO_2

A mass of 4.5 g of 3-(trihydroxy silyl)-1-propanesulfanic acid (SIT) at 35% in water (Gelest) was dissolved in 20 mL of deionized water. At the same time, a mass of 3 g of TiO_2 was mixed with 25mL of deionized water, at 60°C.

The two solutions were slowly mixed together and a 1M of NaOH was added until the mixture reached pH 5.

The mixture was heated to 80°C and it was stirred vigorously by magnetic stirrer for 24h. The process was carried out in the cell reported in Figure 3.1.

The reaction mixture was maintained at 80°C through a silicon oil; a sensor, placed in the solution, monitored temperature during the experiments. High mixing intensity and high concentration of SIT in the aqueous solution have proved to be crucial in achieving the requirements.

Once the reaction was complete,

10mL of suspension were transferred in test tubes of 50mLand the suspension was centrifugated at 4000rpm for 15min, to separate the particles from the solution The solid was washed using 20mL of mixture 30%wt of ethanol (sigma-aldrich, 96%) in deionized water, in order to remove the SIT from the solution. This procedure has been repeated 3 times.

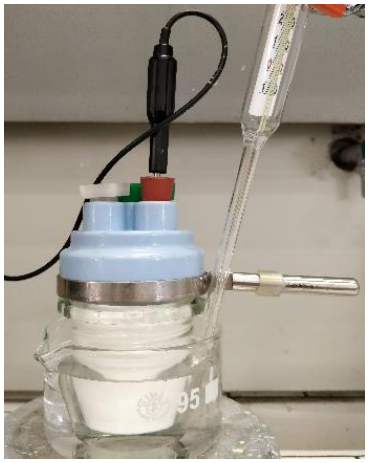

Figure 3.1 *Batch cell used for the surface treatment. Cell is immersed in a bath of silicon oil Two sensors are installed for monitoring oil temperature and reaction mixture temperature.*

After last centrifugation step, particles were dried at 105°C for 60 minutes, at atmospheric pressure.
Propylene Carbonate was added at dry nanoparticles and the suspension was stirred vigorously by magnetic stirrer for 30 minutes and sonicated for 4-5h, maintaining the temperature below 30°C.
The loading of particle in the solvent was varied according the test requirements. Prior to any test, the suspension was re-agitated by bath sonication.

3.1.2 LMNO

In LMNO surface modification process deionized water cannot be used because H_2 could be quickly produced as reported by the following equation (Casellato *et al.*, 2006):

$$\mathrm{Li_{intercalated}} + \mathrm{H_2O} \leftrightarrow \mathrm{Li^+} + \mathrm{OH^-} + 1/2\mathrm{H_2} \qquad 3.1$$

In order to deintercalate Li from the structure, 1.5g of LMNO was dispersed in isopropanol (35mL at least) and maintained stirred by magnetic stirrer.
Deionized water has been added dropwise, under inert gas purge N_2, in order to remove H_2 gas generated. During the process the temperature decrease due to endothermic reaction. The experimental equipment is reported in Figure 3.2a.
As temperature is an indicator of the reaction, addition of water was regulated to maintain temperature of suspension which it is maintained at 15°C.
This procedure allows to reduce the accumulation of H_2 in the solution.
The discharged LMNO particles were treated using the same protocol described in §3.1.1 for titania particles.

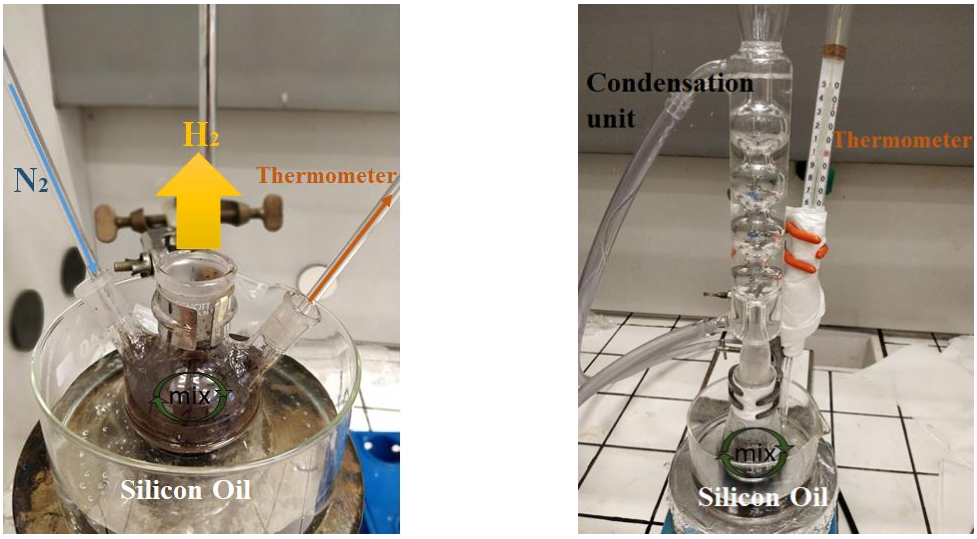

(a) *(b)*

Figure 3.2 *The representation of experimental equipment used for (a) discharging of Li intercalated under inert gas purge $N_2$and (b) surface treatment of LMNO with condensation unit and thermometer*

The treatment was carried out in an open system, shown in Figure 3.2b, equipped with a 250mL round-bottom flask and a unit to condense the vapour. The temperature was maintained constant through a silicon oil bath. This equipment permits to remove $H_{2\ gas}$ generated.

10mL of aqueous suspension were transferred in test tubes of 50mL. The suspension was centrifugated at 9000rpm for 35min to separate the particles from the solution. The particles were washed using 20mL of mixture 30%wt of ethanol (sigma-aldrich, 96%) in deionized water in order to remove to remove the SIT from the solution. This procedure was repeated 3 times.

After last centrifugation step, particles were dried at 105°C for 60 minutes, at atmospheric pressure.

In a general nanofluid preparation procedure, Propylene Carbonate was added to dry nanoparticles and the suspension was stirred vigorously by magnetic stirrer for 30 minutes to achieve homogeneous suspension. The suspension was then sonicated for 4-5h, maintaining the temperature below 30°C.

The nanoparticle concentration in the solvent was varied according the test requirements

Prior to any test the suspension was re-agitated by bath sonication.

3.2 Cycling Voltammetry

Cycling Voltammetry is an electrochemical technique widely used for investigating the electrochemical behaviour of a system. It is usually the first experimental approach performed in an electroanalytic study, since it gives information on redox potentials of electroactive species and on the effect of media on redox process.
In this study, cycling voltammetry has been used to verify the electrochemical activity of the investigated materials and evaluate the mechanisms affecting the electrochemical reactions. Tests were conducted using the electroactive materials dispersed in solution instead of in form of a deposit on electrode because they dissolved in PC.

3.2.1 Cycling Voltammetry technique

The technique consists of varing the working electrode potential linearly along time and recording the resulting current, as reported in Figure 3.3.

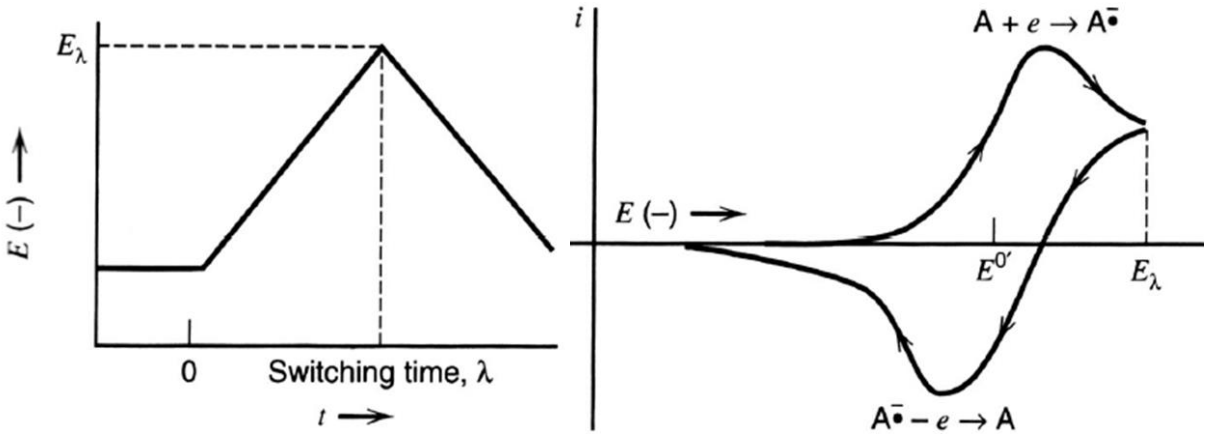

Figure 3.3 *(a) Cyclic potential sweep and (b) resulting cyclic voltammogram. (Electrochemical methods, Allen Bard, 2ªed.)*

If the scan starts at a potential E^i, only capacitive current flows; when the potential reaches the vicinity of E^0, the redox reaction starts and the faradic current flows. Electrode potential continues to grow and the current increases until the surface concentration of the electroactive specie drops nearly to zero.

The mass transfer to the surface reaches a maximum rate. The magnitude of the current is proportional to the concentration of the electroactive species in solution, which allows CV to be used to determine species concentration. A representation is reported in Figure 3.4.

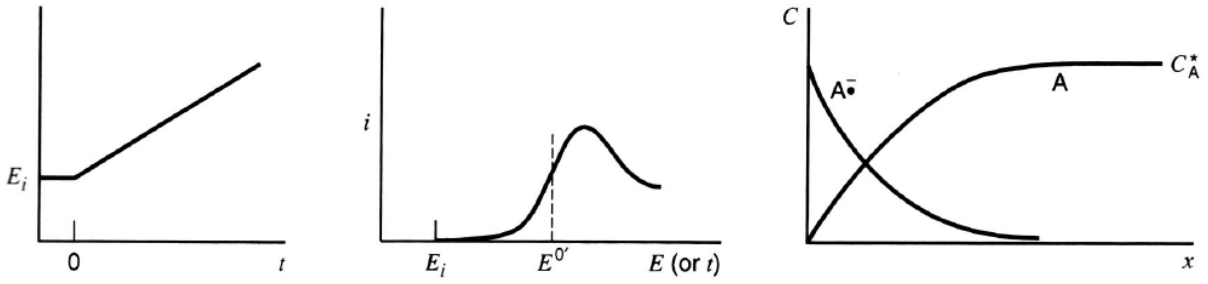

(a) *(b)* *(c)*

Figure 3.4 *(a)Linear potential sweep starting at E_i. (b) Resulting i-E curve. (c) concentration profiles of the oxidized and reduced species. (Electrochemical methods, Allen Bard, 2ªed.)*

The technique is characterized by the rate of voltage change over time, called scan rate (V/s). It is possible to understand if the process is diffusion-limited (3.2) of kinetic-limited (3.3) observing the increasing of peak current with the scan rate.

Diffusion regime $i \sim v^{1/2}$ 3.2

Kinetic regime $i \sim v$ 3.3

Where

i= current intensity [A];

v=scan rate [V/s].

From this technique is possible to get the standard potential of the electrochemical process investigated, understand of the rate determine step (diffusion or kinetic). The equipment required to perform CV tests is composed by a potentiostat connected to three electrodes (work electrode-WE, counter electrode-CE and reference electrodes) immersed in the investigated solution. The potential is applied between the working and reference electrode and, at the same time, the current at the working electrode is measured. Charge flows between the working electrode and the current electrode. Environment of argon (Ar) or some noble gas is preferred.

3.2.2 Experimental procedure

Sample of 40mLof PC 0.5M $LiClO_4$ was prepared. The CV was measured at scan rate of $10mVs^{-1}$and $100mVs^{-1}$ under Argon flow for helping O_2 and gas impurities to go out.

The analyzed nanoparticles were mixed with the medium and then sonicated for 30 minutes, getting a 5%wt suspension of solid in PC 0.5M $LiClO_4$. Before the test, Ar gas flowed through the solution.

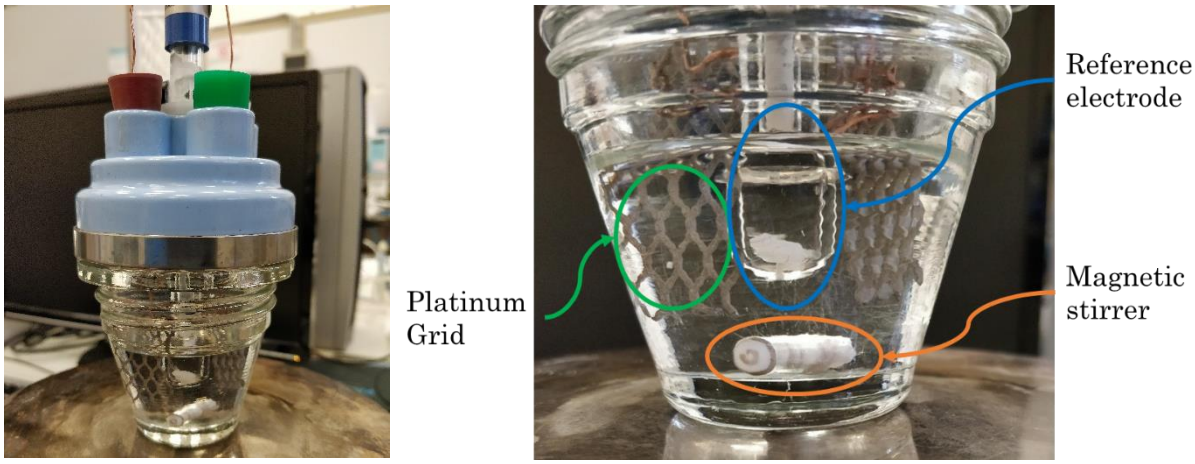

Figure 3.5 *Electrochemical cell used to perform CV and chronoamperometry tests*

Electrochemical tests were conducted using a potentiostat AUTOLAB PGSTAT128N, a titanium platinated grid both as working and counter electrode and Ag/AgCl saturated reference electrode as reported in Figure 3.5.
CVs were performed at scan rate of 10mV/s and 100mV/s.
After each test the mixture was stirred to refresh the material on the surface of WE and CE, while tests were carried out in static environment (no agitation, at room temperature.

3.3 Chronoamperometry

Chronoamperometry is an useful and widely used technique in which a potential step is applied to the working electrode and the resulting current is observed as a function of time.
As reported in Figure 3.6, the system is under potential E_1 until t=0. At this potential where the redox reaction does not start. At time t=0 the potential switch to E_2 and redox reaction starts.

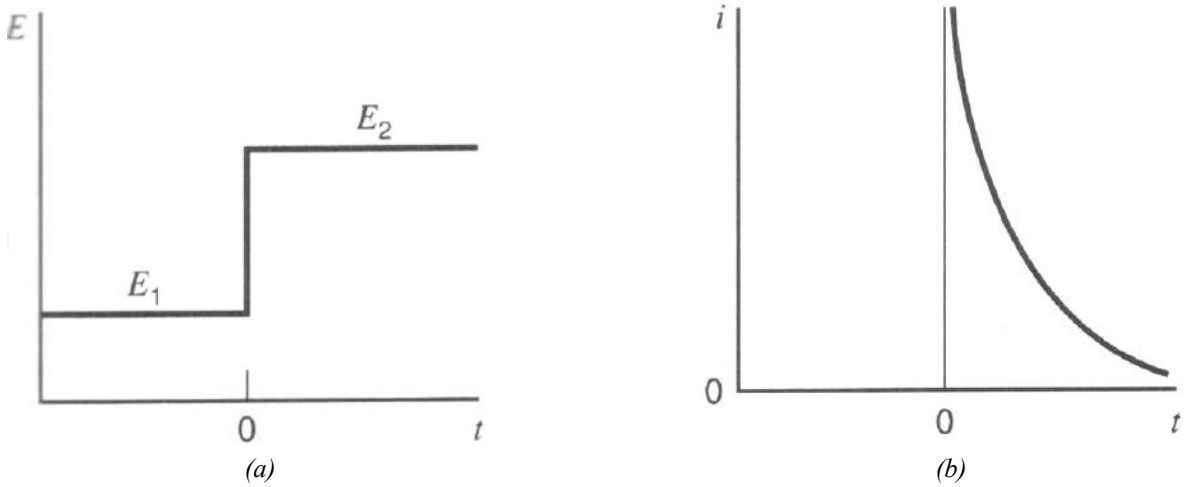

Figure 3.6 *(a) waveform for a step experiment in which the electroactive specie is electroinactive at E1 but is reduced at the diffusion limited rate at E2. (b) Current flow vs.time.*
(Electrochemical methods, Allen Bard, 2ªed.)

At the beginning a capacitive current is delivered showing an initial high current recorded; then the system records only the faradic current delivered by the process occurring at the working electrode. After some time the current is stabilized.
In the system analysed the current delivered depends on the kinetic properties of electroactive species and on frequency of collision between particles and current collector.
To evaluate both rheological and electrochemical properties a chronoamperometry at same level of agitation has been performed to understand the total effects of the surface treatment.

3.3.1 Experimental procedure

The analysis was conducted by using AUTOLAB PGSTAT128N instrument. Tests were performed in an electrochemical cell reported in Figure 3.5. The reference electrode was Ag/AgCl saturated electrode. Current collectors, both working and counter, were made of a titanium platinated grid.
The same cell grids were used for both materials, so the active area is the same for both materials analysed.
The nanofluids were prepared mixing a solution of 40mL of PC 0.5M $LiClO_4$ with nanoparticles material at 5%wt. Before the tests, the nanoparticle suspension was sonicated for 20 minutes.
Prior to any measurement to perform the measurement on new material, the grid was washed with deionized water, and sonicated for 10min. Water was removed with a flux of N_2 at high pressure.
The agitation has been provided by a magnetic stirrer on the bottom.

3.4 Viscosity measurement

The viscosity of suspension was measured using a viscometer Brookfield model DV-III, with spindle “SC4-18” in the “small sampler adapter”.
The suspension is a non-Newtonian fluid and the viscosity varies in time and shear stress.
Nanofluids at 5%vol of solid material (16%wt TiO_2 and 17%wt LMNO) are sonicated for 20min and then the viscosity measurement was performed.
A sample of 8mL of nanofluid was analysed at some specific shear stress for 5 minutes, recording the value of viscosity at t=0s and t=300s.
Before to start a new test at different shear rate, the sample was sonicated to avoid the effects of the shear stress applied during the previous measurement.
During tests, sample temperature was monitored, showing a constant value of 21°C.

Chapter 4

Results

In this chapter it is reported the motivation that leads to perform the experimental study and the relevant results. The final aim is to get some information about the electrochemical behaviour of developed nanofluids and more specifically about surface treatment which is the key factor to improve their performance.

4.1 TiO_2 and TiO_2-S nanofluids

The pristine TiO_2 shows a standard potential E^0 at -1.4V vs NHE (-1.25 vs SCE) and a theoretical capacity of 330mAhg^{-1}, which is a very high value.
Commercially, the nanoparticles are available with a diameter of 15-30nm.
The best choice of nanoparticle material would be a metal oxide with great electrochemical properties and nanometric diameter, as small as possible so as to decrease the viscosity of nanofluids.
The electrochemical behavior and the rheological properties of both TiO_2 and TiO_2-S nanofluids have been evaluated.
A series of tests have been done in order to verify the system designed as described in chapter 2.

4.1.1 Cycling voltammetry

Cycling voltammetry has been performed at different scan rates to check the electrochemical process active in our nanofluids. The analysis has been performed directly to nanofluids in order to verify the electrochemical activity and find out which is the regime of the process, as explained in §3.2.1.
Voltammetry measurements have been performed in a three-electrode electrochemical cell.
The results are reported in Figure 4.1.
From the cycling voltammetry it has been verified that the electrochemical activity of the designed nanofluids. Standard potential E^0 is equal -1.25V vs Ag/AgCl.
As it can be noticed in Figure 4.1 the degradation of the solvent starts at potential E= -2V vs Ag/AgCl.

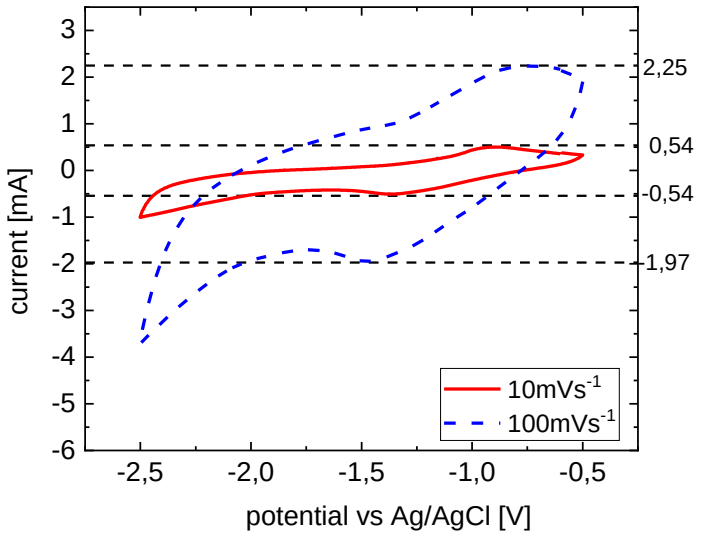

Figure 4.1 *Cycling voltammetry of the nanofluid based on TiO2 (surface treated) in PC 0.5MLiClO₄ at scan rate of 10mVs⁻¹ and 100mVs⁻¹. Second cycles.*

The peak currents increase with increasing scan rate. For perfect diffusion limited-process the ratio between the current peaks shall be equal to $\sqrt{100/10}$, instead of 100/10 relevant to the kinetic-limited process, as explained in §3.2.1.

As it can be noticed inFigure 4.2, the point of the anodic peak matches the theoretical diffusion limited line with good tolerance while there is a discrepancy with the theoretical line in the case of cathode peak. The reason is that the time needed to achieve some specific potential in cycling voltammetry at $10mVs^{-1}$ is higher than $100mVs^{-1}$. Settling phenomenon depends on the time for the same system. In CV at $10mVs^{-1}$ settling is more evident in the system, thus most of current collector surface is in contact only with solvent.

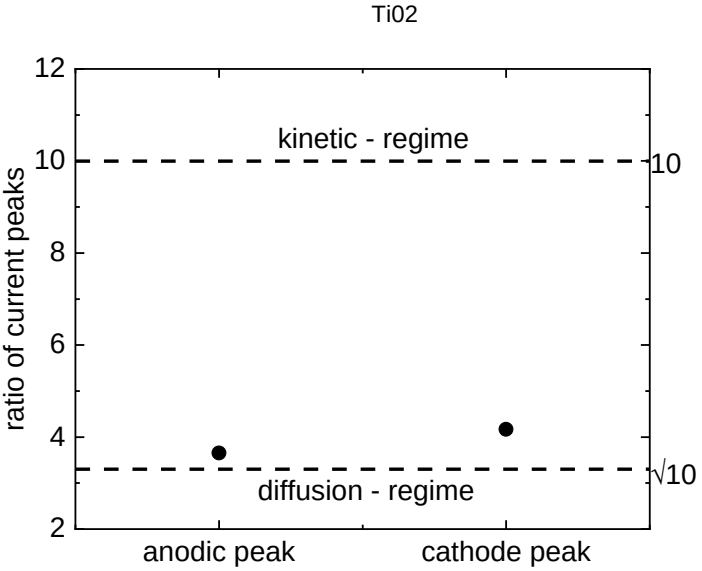

Figure 4.2 *Square root of ratio of current peaks vs the potential. Theoretical diffusion and kinetic regime lines and experimental points. Data related to CV of TiO_2 nanofluid in PC 0.5M $LiClO_4$*

This phenomenon decreases the resulting current, getting a ratio between the current peak of curves slightly higher than the theoretical one.

According to the results, the electrochemical process of intercalation can be considered diffusion-limited.

The same procedure has been used to analyze the behavior of the TiO_2-S based nanofluid.

Cycling voltammetry confirms the electrochemical activity of the treated nanoparticle in PC. 0.5M $LiClO_4$ at E^0 equal to -1.2Vvs Ag/AgCl, as shown in Figure 4.3.

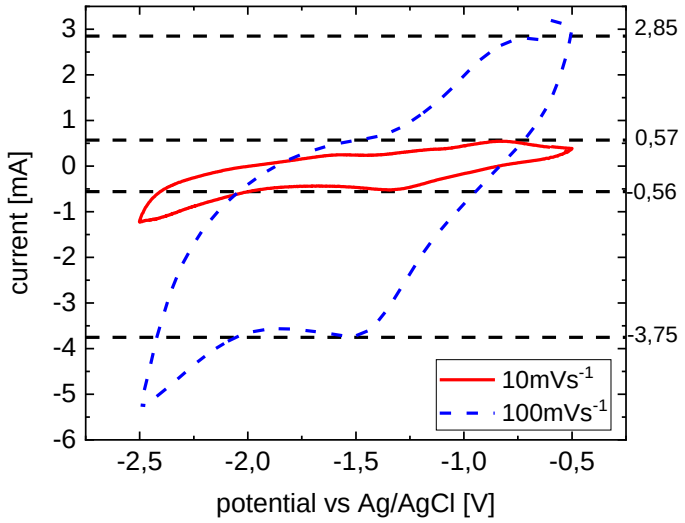

Figure 4.3 *Cycling voltammetry of the nanofluid based on TiO2-S (surface treated) in PC 0.5MLiClO4. at 10mVs^{-1} and 100mVs^{-1} Second cycles.*

As it can be noticed in Figure 4.4 , the ratio between the peaks of the two curves is higher than the value obtained for the TiO_2 , reported in Figure 4.2.

In the case of TiO_2-S particles, suspension is stable due to the surface treatment, so the settling phenomenon has no effects on CV.

When the particle are actively colliding with the current collector, the potential permits the intercalation into the lithium particle near the contact surface.

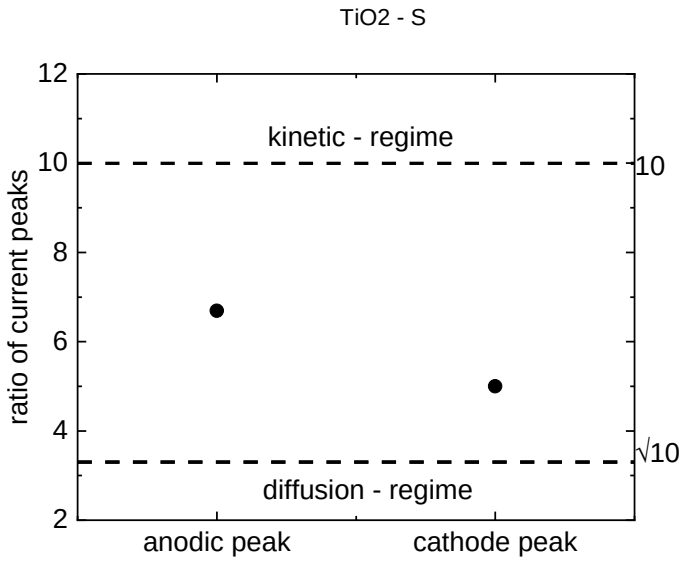

Figure 4.4 *Square root of ratio of current peaks vs the potential around the peak in CV. Theoretical diffusion and kinetic regime lines and experimental points. Data related to CV of TiO_2-S nanofluid in PC 0.5M $LiClO_4$.*

There are 2 different processes providing lithium ion on the contact surface between the current collector and the particle: the lithium ion can move from bulk to particle or from the bulk to current collector surface. A schematic representation of the processes is reported in Figure 4.5. In the case of TiO_2 particles, the rate of electron transfer is fast compared to the rate of mass transport and it doesn't control the overall rate of the process, see Figure 4.2. When treated particles (TiO_2-S) are used, the transport process from bulk to particle changes due to the surface modification occurred. The mass transport from bulk to the particle surface depends on the concentration gradient and on the electrostatic attraction between the negative layer and positive lithium ion. When treated particles are used, the electrostatic contribution increases the transport rate making it comparable or competitive with the rate of charge transfer, so turn the regime.

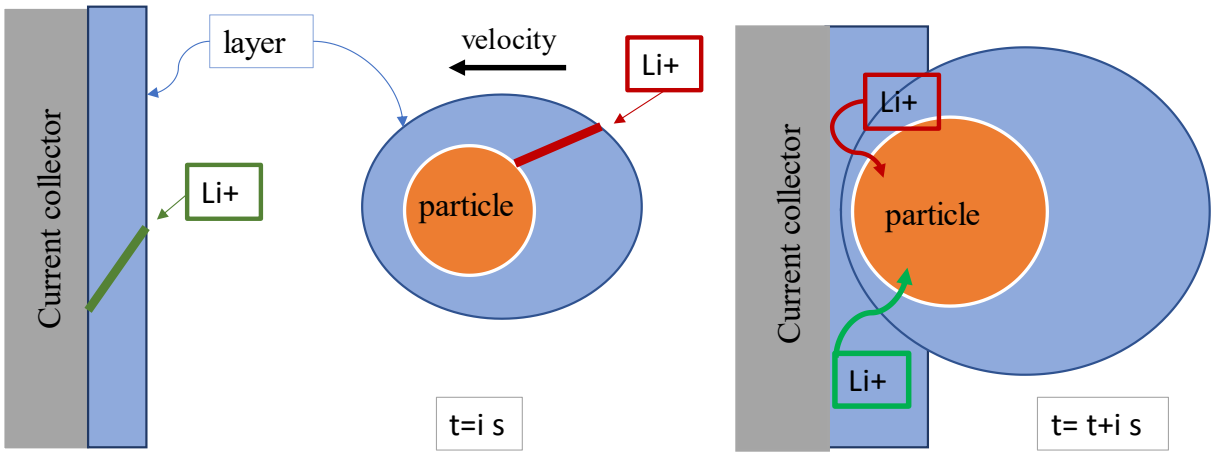

Figure 4.5 *Schematic representation of the processes providing lithium ions near the surface of contact between particle and current collector.*

The observed current is controlled by both mass transport and charge transfer kinetics. This mixed regime explains why the value of experimental ratio is in the middle region between diffusion and kinetic limited regimes, as shown in Figure 4.4.

Figure 4.3 highlights higher activity of the anodic peak than the cathodic one, particularly when a scan rate of $100mVs^{-1}$ is used. This effect is not present in nanofluid with TiO_2 particles.

The presence of a negative layer around the treated particle creates an high concentration of Li^+ around the outer surface of the solid. In the inner surface, between the negative layer and TiO_2 particle surface, no lithium ions are present at the beginning.

The available lithium ions around the particle are intercalated when the particle collides with the current collector, under an anodic potential.

At cathodic potential the deintercalation process happens. At the beginning the Li^+ ions exit from the solid but they stay between surface of particle and negative layer, as reported in Figure 4.6. The Li^+ ions start to exit from the coating when the concentration of Li^+ ions between the

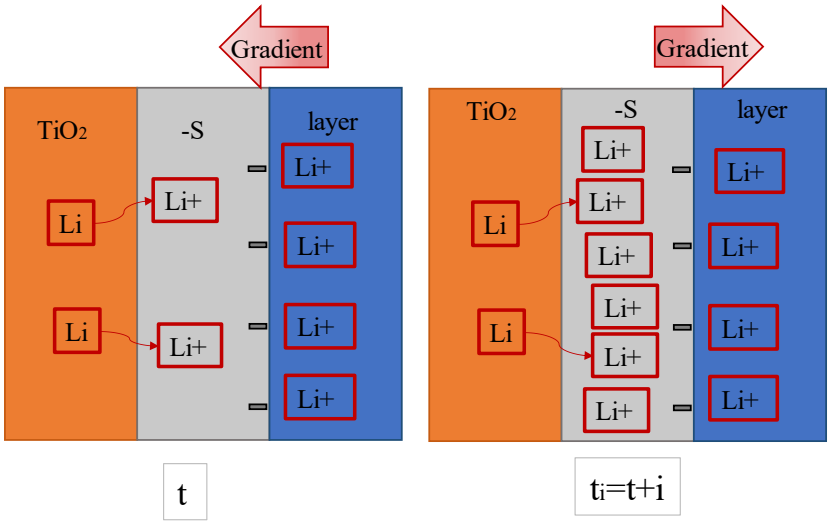

Figure 4.6 *Schematic representation of the transition state of diffusion of lithium ions during the deintercalation process.*

particle and the negative layer overcomes the outer concentration. This diffusive transport needs a certain time to start and its effect is more evident at high scan rate because the system has less time available to stabilize.

At scan rate of $10mVs^{-1}$ the system reaches this equilibrium before to achieve the stop of the test or the degradation of the solvent. For this reason, the difference from cathodic and anodic effects is negligible.

The delay in Li diffusion affects the mass transfer step, improving its role in the intercalation rate, as shown in Figure 4.4.

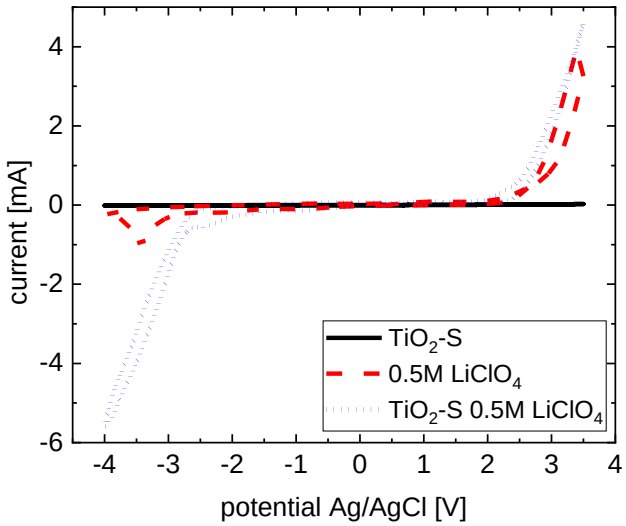

Figure 4.7 *Cycling voltammetry of 3 fluids at 50mV. All fluids are based on propylene carbonate.*

During the CV investigation on the material, it has been noticed that degradation of the solvent starts before when the intercalation process happens. In Figure 4.7 there is the evidence of what above described. In TiO_2 nanofluid this phenomenon doesn't appear.

The solvent shows a short window of stability only when TiO_2-S and $LiClO_4$ are present together.

This behaviour is due to the high current through the surface between particle and current collector and negative layer of particle. This is due to the electrostatic forces that polarize the solvent helping the degradation. This aspect needs to be deeply investigated.

4.1.2 Rheological properties

In order to evaluate the rheological properties, viscosity measurements have been carried out. Viscosity gives an information about the pumping energy required.

Measurements of viscosity at different shear rate has been performed.

The nanofluids analysed showed a non-Newtonian behaviour. As it can be noticed in Figure 4.8, the surface treatment allows to reduce the viscosity of the nanofluid, getting the possibility to decrease the energy loss in pumping.

Measurements at time t=0 and t=300s have ben considered, when the viscosity value is stabilised.

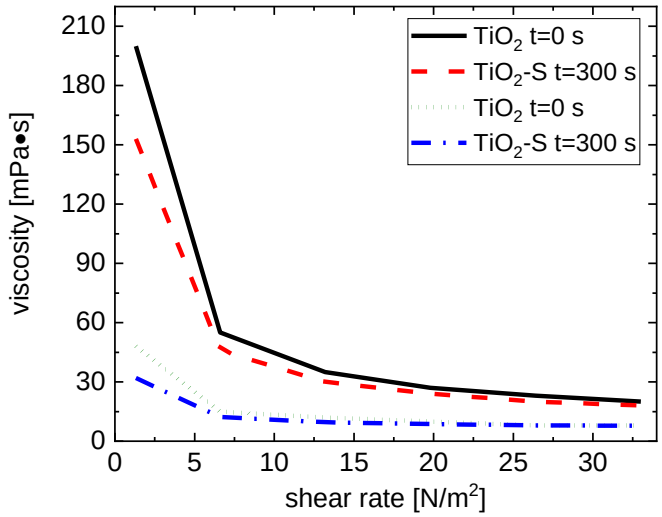

Figure 4.8 *Viscosity of TIO₂ at 5%vol in PC nanofluid for different shear rate at time t=0 and t=300s.*

These fluids show a very complex rheological behaviour, depending strongly on time and shear rate. In particular, the TiO_2-S based nanofluid shows slightly less shear rate dependence compared with the pristine material.

4.1.3 Chronoamperometry

A chronoamperometry on nanofluid at some specific mixing condition has been carried out. The current obtained depends on the properties of electroactive material and on the frequency of collision between particle and current collector, and therefore from the rheological behaviour of the nanofluid.

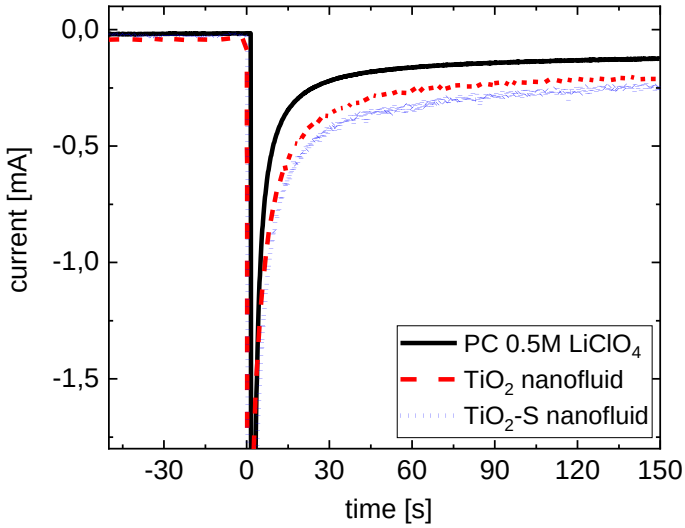

Figure 4.9 *Chrono amperometry of 3 system at -1V vs Ag/AgCl until t=0 and -1.6V vs Ag/AgCl after t=0. Mixing condition are provided with magnetic stirrer.*

The surface treatment decreases the viscosity of the fluid and the coating influence the kinetic/diffusion properties of the particles.
In order to evaluate the total effect of the surface treatment on the system performance, a chronoamperometry at -1.6V vs Ag/AgCl has been carried out
The potential applied has been chosen based on CV analysis Figure 4.1 and Figure 4.3.
A potential more negative than anodic peak has been applied to take into account the overpotential and achieve condition that enables the intercalation process.
In this case, keeping the same energy for mixing, it has been found which nanofluid gives higher current. The selected nanofluids are at 5%wt.
In Figure 4.9 it has been reported the resulting current for solvent (PC at 0.5M $LiClO_4$), TiO_2 nanofluid and TiO_2-S nanofluid.
TiO_2-S nanofluid is the best solution because it gives higher current for the same energy spent to mix.
The average resulting current for TiO_2-S nanofluid is 58% higher than TiO_2 nanofluid if it is considered the contribution given by the solvent. The percentage is calculated according to the equation 4.1

$$\frac{i_{TiO_2-S}-i_{solvent}}{i_{TiO_2}-i_{solvent}} \qquad 4.1$$

where
i= current recorded from the test.
The final average values are reported in Table 4.1.

Table 4.1 *Mean values of the recorded current in the last 10s for the analysed fluids*

Solvent [mA]	**TiO_2 [mA]**	**TiO_2-S [mA]**
-0.125	-0.208	-0.247

At this loading and for this material, the contribution of the current generated by the solvent is important and it cannot be neglected when comparing the behaviour of the nanofluids.
It has been assumed that the contribution on current by solvent is the same in all the nanofluids.

4.2 LMNO and MNO-S nanofluids

The LMNO is a widespread material in Li-ion battery.

For Li ion intercalated material, the preparation of nanofluids has been carried out using a different procedure, divided in 2 steps.

The aim of the first step is to deintercalate the lithium from the particles; LMNO is converted in MNO following the reaction reported in equation 3.1.

$$Li_{intercalated} + H_2O \leftrightarrow Li^+ + OH^- + 1/2H_2 \qquad 3.1$$

This step creates the right conditions to the second step, which shall be done in the deionized water.

The second step consists of treating MNO nanoparticles to produce MNO-S material.

Experimental investigation has been performed on pristine material, LMNO, discharged material MNO, and the surface treated MNO-S.

All compounds have been analysed by cycling voltammetry and viscosity measurements.

This paragraph has been divided into sub-paragraphs describing each single step.

4.2.1 From LMNO to MNO

In Figure 4.10 CVs of both pristine LMNO and discharged material MNO at scan rate of 10mVs^{-1} are reported. Attention is focused on the deintercalation process.

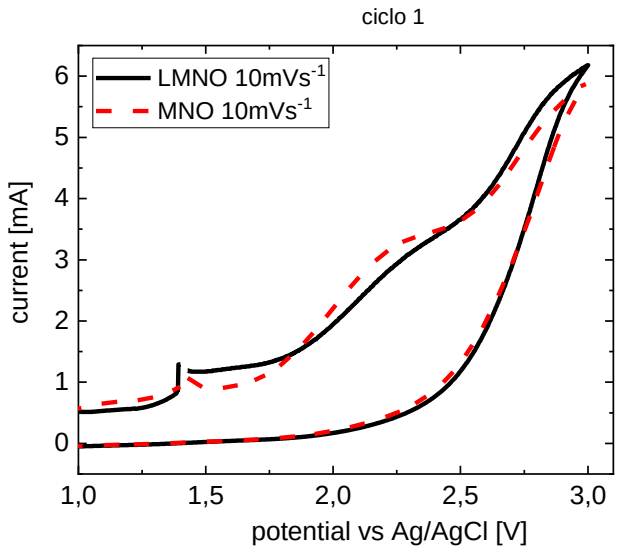

Figure 4.10 *CV of pristine LMNO and MNO particles in PC 0.5M $LiClO_4$ at scan rate of 10mVs^{-1}.*

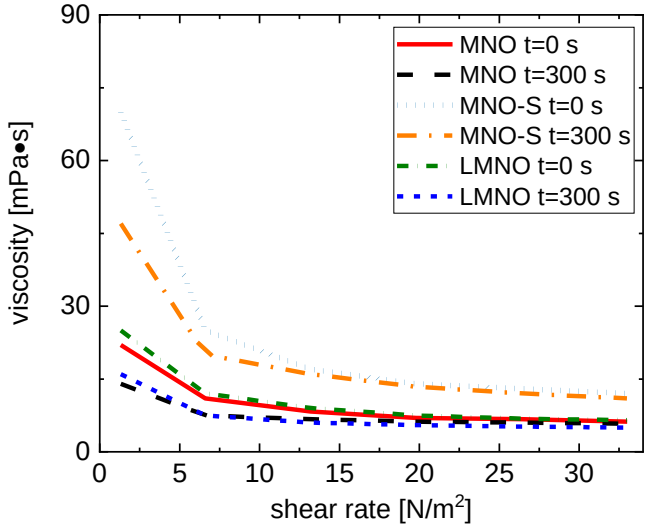

Figure 4.11 *Viscosity measurement of nanofluids with particle loading of 5%vol of LMNO, MNO, MNO-S based on PC solvent. Measurement for each nanofluid has been performed at time t=0s and t=300s.*

It would expect that MNO shows a weak deintercalation peak, but only the intercalation one. This result suggests that some lithium is present in the particle. Therefore, during the discharging reaction metal ions are partially removed from the host material and for this reason, the deintercalation process is very similar to LMNO. To understand the underlying mechanisms in this process in more detail, the discharging treatment shall be deeper investigated.

Results of viscosity measurement are reported in Figure 4.11. Tests have been performed on nanofluids with particle loading of 5%vol. As expect, the fluids show a similar behaviour, indicating that the deintercalation doesn't affect viscosity.

4.2.2 From MNO to MNO-S

In order to evaluate the applicability of the surface treatment on the material obtained by the discharging process, MNO-S particles have been prepared following the procedure described in 3.1.2.

CVs have been performed on surface–modified material and the results are reported in Figure 4.12. No electrochemical activity has been detected.

It can be concluded that surface treatment has compromised the electrochemical activity of the material.

The viscosity measurement shows an increasing of viscosity instead of a decreasing as reported in Figure 4.11.

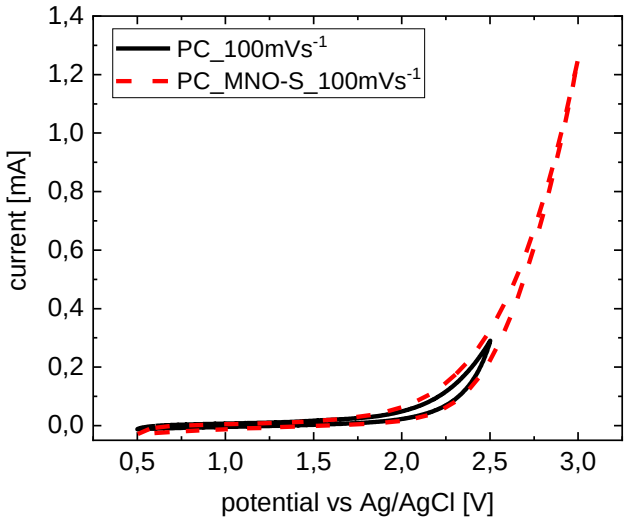

Figure 4.12 *CV of MNO-S nanofluid and solvent (PC) in comparison. The scan rate is equal to 100mVs^{-1} and working current collector is glassy carbon.*

During the treatment, the equilibrium of reaction of discharging (equation 3.1) is translated to the right due to the increase in temperature. The consequence is the delivering H_2 in the solution. The presence of H_2 in the solution causes the reduction of sulphurous group of SIT in hydroxyl group, as reported in equation 4.2.

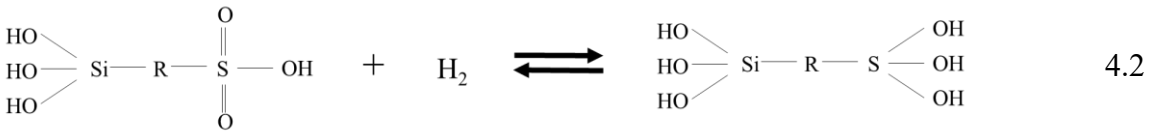

The resultant molecule has 6 hydroxyl group, two of which are new.

The solution condition facilitates the condensation reaction because the process has been though for permitting the condensation reaction between the hydroxyl group of particles and the one of SIT.

SIT reduced molecules link to each other by a condensation reaction as reported in equation 4.3 and equation 4.4.

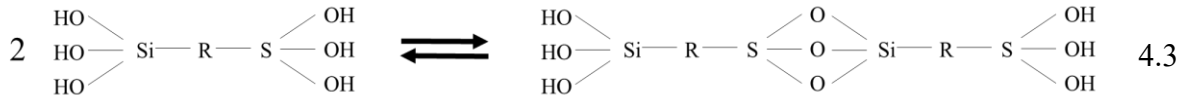

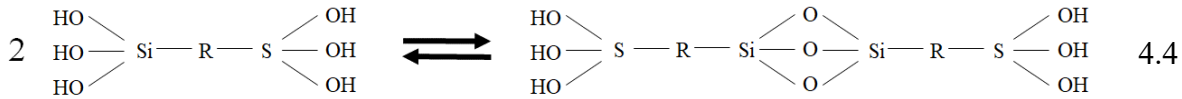

This phenomenon gives a product long chain of SIT modified molecules, couple of linked particle and network of SIT modified molecules, as reported in Figure 4.13.

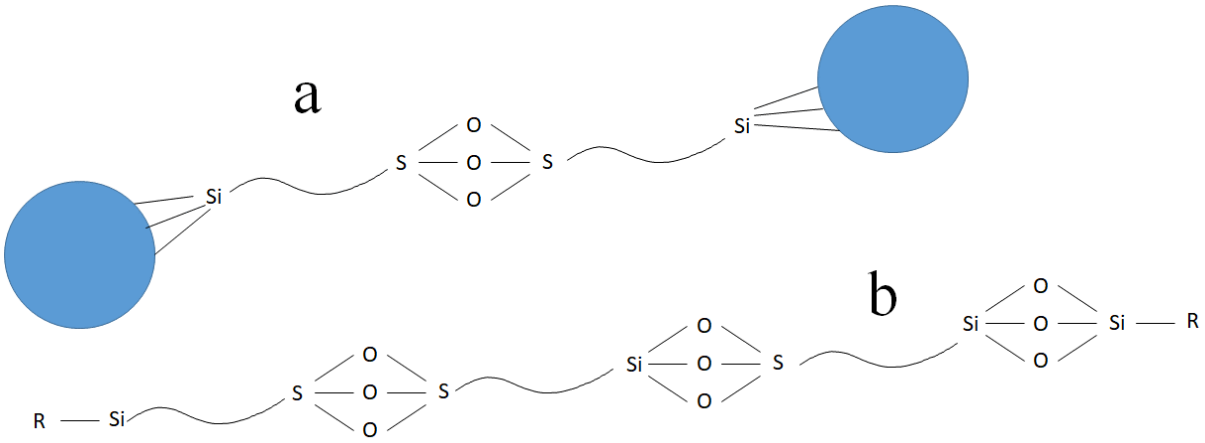

Figure 4.13 *Possible product of the condensation reaction between SIT reduced molecules. (a) 2 particles linked through a chain of SIT. (b) an example of long chain composed by SIT reduced molecules*

The long chain and the particle bound to each other could be responsible for the increase in viscosity.

The complex rheological behaviour of nanofluid and the uncertainty in the discharge process suggest deeper investigation to optimize the preparation procedure.

Conclusions

The aim of the Thesis is to develop and to analyse two nanofluids for redox flow battery applied on electrical vehicle.

The developed nanofluids are based on propylene carbonate 0.5M $LiClO_4$ solvent for its excellent stability over a wide voltage range

TiO_2 and LMNO materials in nanoparticle form have been selected.

A surface treatment has been done to decrease the viscosity of solution reducing the energy loss in pumping. The positive effect on viscosity is due to a negative layer that covers the particles causing a repulsive force between them.

Both rheological and electrochemical tests have been performed on pristine and treated materials.

TiO_2 modified shows a higher electrochemical activity than pristine material, in particular with reference to the lithium intercalation process. There are two paths to provide/remove the lithium ion in the intercalation/deintercalation process: from bulk to current collector surface (and vice versa) and from bulk to particle surface (and vice versa). The negative layer on the surface of treated particle attracts the lithium ions around the particle increasing the mass transport rate from bulk to the particle surface. Electrochemical reaction mechanisms have been analysed for both TiO_2 based nanofluids. In particular, it has been noticed that both the kinetic and diffusive regimes make a contribution to the observed current when the surface modified particles are used.

The current in redox flow battery depends on electrochemical properties and on the frequency of collision between particles and current collector, and therefore from the rheological behaviour of the nanofluid.

A chronoamperometry takes into account the total effects of surface modification. The modified TiO_2 shows average resulting current 58% higher than the pristine material for the same energy spent in mixing.

These results confirm the positive effect of the treatment on nanofluids performance.

LMNO material has been treated in isopropanol and aqueous solution before the surface modification step, for discharging intercalated lithium and avoiding hydrogen generation due to the reaction with water.

The discharged material shows a significant deintercalation activity, indicating that during the deintercalation reaction metal ions are partially removed from the host material.

The surface treatment has been done on discharged material and the deintercalation process has been investigated. During the treatment at 80°C in aqueous solution some hydrogen has been generated.

The molecules used to modify the surface of particles have been reduced by hydrogen. The sulphurous group became to hydroxyl group. These new molecules reacted creating long chains which bind the particles to each other. The new structure could be responsible for the observed increase in viscosity and the turning off of particle electrochemical activity.

This thesis investigated and demonstrated that the surface treatment allows to obtain nanofluids with low viscosity while simultaneously retaining electrochemical activity of the nanoparticles.

TiO_2 doesn't shows high conductivity and better anodic material like LTO could be tested.

The preparation procedure for lithium intercalated materials shall be optimized in order to retain the electrochemical properties in the final nanofluid. In particular, a deep electrochemical discharge of the material would be considered.

A study to maximize the effect of the lithium salt on donor number could help to obtain nanofluids with low viscosity at high particle loading.

A new solvent composed by two chemicals could be considered to increase window stability and donor number.

References

Casellato, U., Comisso, N., & Mengoli, G. (2006). Effect of Li ions on reduction of Fe oxides in aqueous alkaline medium. *Electrochimica Acta*.

Chen, X., Hopkins, B., Helal, A., Fan, F., Smith, K., Li, Z., . . . Chiang, Y. (2016). A low-dissipation, pumpless, gravity-induced flow battery. *Energy and Environmental Science*.

Curtis, C., Wang, J., & Schulz, D. (2004). Preparation and Characterization of LiMn 2 O 4 Spinel Nanoparticles as Cathode Materials in Secondary Li Batteries. *Journal of The Electrochemical Society, 151*, 590-598.

Ding, M., & Richard Jow, T. (2004). How Conductivities and Viscosities of PC-DEC and PC-EC Solutions of LiBF[sub 4], LiPF[sub 6], LiBOB, Et[sub 4]NBF[sub 4], and Et[sub 4]NPF[sub 6] Differ and Why. *Journal of The Electrochemical Society*.

Doi, T., Inaba, M., Tsuchiya, H., Jeong, S.-K., Iriyama, Y., Abe, T., & Ogumi, Z. (2008). Electrochemical AFM study of LiMn 2 O 4 thin film electrodes exposed to elevated temperatures. *Journal of Power Sources, 180*, 539-545.

Duduta, M., Ho, B., Wood, V., Limthongkul, P., Brunini, V., Carter, W., & Chiang, Y. (2011). Semi-solid lithium rechargeable flow battery. *Advanced Energy Materials*.

Fan, F., Woodford, W., Li, Z., Baram, N., Smith, K., Helal, A., . . . Chiang, Y. (2014). Polysulfide flow batteries enabled by percolating nanoscale conductor networks. *Nano Letters*.

Huang, Q., Li, H., Grätzel, M., & Wang, Q. (2013). Reversible chemical delithiation/lithiation of LiFePO ₄ : towards a redox flow lithium-ion battery. *Phys. Chem. Chem. Phys.*

Huang, X., Lv, D., Zhang, Q., Chang, H., Gan, J., & Yang, Y. (2010). Highly crystalline macroporous β-MnO2: Hydrothermal synthesis and application in lithium battery. *Electrochimica Acta*.

Katsoudas, J., Timofeeva, E., Segre, C., & Singh, D. (s.d.). Integration of Flow Batteries into Electric Vehicles: Feasibility and the Future.

Li, Z., Smith, K., Dong, Y., Baram, N., Fan, F., Xie, J., . . . Chiang, Y. (2013). Aqueous semi-solid flow cell: Demonstration and analysis. *Physical Chemistry Chemical Physics*.

Liu, G., Wen, L., & Liu, Y. (2010). Spinel LiNi 0.5Mn 1.5O 4 and its derivatives as cathodes for high-voltage Li-ion batteries. *Journal of Solid State Electrochemistry*.

Montoto, E., Nagarjuna, G., Hui, J., Burgess, M., Sekerak, N., Hernández-Burgos, K., . . . Rodríguez-López, J. (2016). Redox Active Colloids as Discrete Energy Storage Carriers. *Journal of the American Chemical Society*.

Mubeen, S., Jun, Y., Lee, J., & McFarland, E. (2016). Solid Suspension Flow Batteries Using Earth Abundant Materials. *ACS Applied Materials and Interfaces*.

Pan, F., Huang, Q., Huang, H., & Wang, Q. (2016). High-Energy Density Redox Flow Lithium Battery with Unprecedented Voltage Efficiency. *Chemistry of Materials*.

Pan, F., Yang, J., Huang, Q., Wang, X., Huang, H., & Wang, Q. (s.d.). Redox Targeting of Anatase TiO 2 for Redox Flow Lithium-Ion Batteries.

Qi, Z., & Koenig, G. (2016). A carbon-free lithium-ion solid dispersion redox couple with low viscosity for redox flow batteries. *Journal of Power Sources*.

Qi, Z., & Koenig, G. (2017). Review Article: Flow battery systems with solid electroactive materials. *Journal of Vacuum Science & Technology B, Nanotechnology and Microelectronics: Materials, Processing, Measurement, and Phenomena*.

Robinson, J., & Koenig, G. (2015). Tuning solution chemistry for morphology control of lithium-ion battery precursor particles. *Powder Technology*.

Sen, S., Chow, C., Moazzen, E., Segre, C., & Timofeeva, E. (2017). Electroactive nanofluids with high solid loading and low viscosity for rechargeable redox flow batteries. *Journal of Applied Electrochemistry*.

Sen, S., Govindarajan, V., Pelliccione, C., Wang, J., Miller, D., & Timofeeva, E. (s.d.). Surface Modification Approach to TiO 2 Nanofluids with High Particle Concentration, Low Viscosity, and Electrochemical Activity.

Sen, S., Moazzen, E., Aryal, S., Segre, C., & Timofeeva, E. (2015). Engineering nanofluid electrodes: controlling rheology and electrochemical activity of γ-Fe2O3nanoparticles. *Journal of Nanoparticle Research*.

Tang, W., Yang, X., Liu, Z., & Ooi, K. (s.d.). *Preparation of b-MnO 2 nanocrystal/acetylene black composites for lithium batteries.*

Timofeeva, E., Katsoudas, J., Segre, C., & Singh, D. (s.d.). Rechargeable Nanofluid Electrodes for High Energy Density Flow Battery.

Ventosa, S., Ventosa, E., Buchholz, D., Klink, S., Flox, C., Chagas, L., . . . Morante, J. (2015). As featured in: Non-aqueous semi-solid flow battery based on Na-ion chemistry. P2-type Na x Ni 0.22 Co 0.11 Mn 0.66 O 2 –NaTi 2 (PO 4) 3. *Chem. Commun, 51*.

Wei, T., Fan, F., Helal, A., Smith, K., McKinley, G., Chiang, Y., & Lewis, J. (2015). Biphasic Electrode Suspensions for Li-Ion Semi-solid Flow Cells with High Energy Density, Fast Charge Transport, and Low-Dissipation Flow. *Advanced Energy Materials*.

Winsberg, J., Hagemann, T., Janoschka, T., Hager, M., & Schubert, U. (2017). Redox-Flow Batteries: From Metals to Organic Redox-Active Materials. *Angewandte Chemie - International Edition*.

Zhang, W.-J. (2010). Structure and performance of LiFePO 4 cathode materials: A review. *Journal of Power Sources, 196*, 2962-2970.

Zhao, X., Wang, J., Dong, X., Liu, G., Yu, W., & Wang, L. (2014). Structure Design and Performance of LiNi x Co y Mn 1-x-y O 2 Cathode Materials for Lithium-ion Batteries: A Review.